



저작자표시-비영리-변경금지 2.0 대한민국

이용자는 아래의 조건을 따르는 경우에 한하여 자유롭게

- 이 저작물을 복제, 배포, 전송, 전시, 공연 및 방송할 수 있습니다.

다음과 같은 조건을 따라야 합니다:



저작자표시. 귀하는 원저작자를 표시하여야 합니다.



비영리. 귀하는 이 저작물을 영리 목적으로 이용할 수 없습니다.



변경금지. 귀하는 이 저작물을 개작, 변형 또는 가공할 수 없습니다.

- 귀하는, 이 저작물의 재이용이나 배포의 경우, 이 저작물에 적용된 이용허락조건을 명확하게 나타내어야 합니다.
- 저작권자로부터 별도의 허가를 받으면 이러한 조건들은 적용되지 않습니다.

저작권법에 따른 이용자의 권리는 위의 내용에 의하여 영향을 받지 않습니다.

이것은 [이용허락규약\(Legal Code\)](#)을 이해하기 쉽게 요약한 것입니다.

[Disclaimer](#)

工學博士學位論文

**Synthesis, characterization, and applications
of poly(olefin ketone) and composites having
excellent mechanical properties.**

우수한 기계적 물성을 가지는 폴리올레핀케톤
고분자와 고분자 복합재료의 합성, 분석 및
응용에 관한 연구

2012年 08月

서울대학교 大學院

化學生物工學部

曹 海 碩

**Synthesis, characterization, and applications of
poly(olefin ketone) and composites having excellent
mechanical properties.**

by

Haesouk Cho

Advisor: Professor Jong-Chan Lee, Ph. D.

**Submitted in Partial Fulfillment
of the Requirements for the Degree of
DOCTOR OF PHILOSOPHY**

August, 2012

**School of Chemical and Biological Engineering
College of Engineering
Graduate School
Seoul National University**

Abstract

Polyketone is the alternating copolymer of carbon monoxide and olefin monomer units. The copolymer itself has been known for over 40 years, but efficient methods for preparing it are a much more recent development. The terpolymer that contains 6wt% propylene in addition to the ethylene and carbon monoxide were also developed recently. The reaction parameters of polyketone polymerization are well known by Shell Oil Company, BP, and Hyosung. The mechanism of polymerization is described briefly and the effect of reaction temperature and time on LVN, Molecular weight, and Bulk Density(BD) is reported and the direct correlation between LVN and Melting Index(MI) is also described.

Fibers of poly(1-oxotrimethylene) which is called copolymer having different draw ratios were prepared and characterized using differential scanning calorimetry (DSC), X-ray diffraction, and universal testing machine (UTM). Tensile strength and modulus of poly(1-oxotrimethylene) fibers having a draw ratio of 16 obtained by drying at 220 °C were found to be 13.4 and 369.8 g/denier, respectively. These values are much larger than those of poly(ethylene terephthalate) (PET) and Nylon 6 fibers that are currently used as tire cords.

Polyketone terpolymer having excellent mechanical properties was also synthesized and composite materials of polyketone containing polyurethane/amino silane functionalized glass fibers were prepared. The compatibilities between the functionalized

glass fiber and the polymer were characterized by observing the fracture surfaces of the composites using scanning electron microscopy (SEM). Mechanical properties of composites with different content, diameter, length, and binder of glass fiber were also studied using universal testing machine (UTM). The introduction of suitably functionalized glass fiber into the polyketone produces composite materials having excellent mechanical properties and they are very promising alternative materials for the engineering plastic applications.

Key words: polyketone, poly(1-oxotrimethylene), fiber, draw ratio, crystallinity, polymer with functionalized glass fiber.

Student Number: 2007-30281

TABLE OF CONTENTS

Abstract	i
List of Figures	v
List of Tables	vi

Chapter 1

Introduction

1.1. Palladium-Catalyzed Alternating Copolymerization and Terpolymerization of Alkenes and Carbon Monoxide	2
1.2. Poly(1-oxotrimethylene) Fibers Prepared by Different Draw Ratios for the Tire Cord Application	9
1.3. Preparation and Properties of Glass Fiber-Reinforced Poly(olefin ketone) Composites	11
1.4. Survey of this Thesis	14
1.5. References	15

Chapter 2

Palladium-Catalyzed Alternating Copolymerization and Terpolymerization of Alkenes and Carbon Monoxide

2.1. Introduction	20
2.2. Experimental	21
2.3. Results and Discussion	37
2.4. Conclusions	39

2.5. References	48
-----------------	----

Chapter 3

Poly(1-oxotrimethylene) Fibers Prepared by Different Draw Ratios for the Tire Cord Application

3.1. Introduction	50
3.2. Experimental	52
3.3. Results and Discussion	56
3.4. Conclusions	63
3.5. References	74

Chapter 4

A Study on the Preparation and Characteristics of Glass Fiber-Reinforced Polyolefin Ketone Composites

4.1. Introduction	77
4.2. Experimental	80
4.3. Results and Discussion	84
4.4. Conclusions	93
4.5. References	100

Abstract in Korean	101
---------------------------	-----

List of Figures

Figure 2-1.	The Flow Diagram of polymerization process	42
Figure 2-2.	The LVN as a function of the reaction temperature	43
Figure 2-3.	The Molecular Weight as a function of the reaction temperature	44
Figure 2-4.	The scanning electron microscopy (SEM) images of the influence of the reaction temperature to particle size	45
Figure 2-5.	The Bulk Density(BD) as a function of the reaction temperature	46
Figure 2-6.	The effect of melting index(MI) on LVN	47
Figure 3-1.	Changes in tensile strength with respect to draw ratio at different drying temperatures	67
Figure 3-2.	Cross-sectional SEM photographs of POTE fibers (a) before and (b) after drying at 220 °C	68
Figure 3-3.	DSC thermograms of POTE-Xs	69
Figure 3-4.	X-ray diffraction patterns of (a) POTE-Xs at room temperature and those of (b) POTE-7 and (c) POTE-16 at different temperatures.	70
Figure 3-5.	Two-dimensional X-ray diffraction photograph of POTE-Xs: (a) powder POTE, (b) POTE-0, (c) POTE-7, (d) POTE-10, (e) POTE-14, (f) POTE-16 at room temperature.	72
Figure 3-6.	Changes in crystallinity and crystalline orientation with respect to draw ratio	73
Figure 4-1.	Synthesis of poly(olefin ketone) terpolymer.	96
Figure 4-2.	¹ H NMR spectra of poly(olefin ketone) terpolymer.	97
Figure 4-3.	Palladium activity and intrinsic viscosity as a function of polymerization temperature	98
Figure 4-4.	SEM images of glass fiber reinforced poly(olefin ketone) composites,	99

List of Tables

Table 2-1.	Reaction Parameter of Polyketone polymerization	40
Table 2-2.	The reaction parameters of Polyketone product specific.	41
Table 3-1.	Drawing conditions, molecular weight, polydispersity index and thermal properties of POTE-Xs	64
Table 3-2.	X-ray results of POTE-Xs	65
Table 3-3.	Mechanical properties of POTE-Xs and commercial fibers	66
Table 4-1.	Characteristics of Glass Fibers used in this Work	94
Table 4-2.	Mechanical Properties of Poly(olefin ketone) Terpolymer, Glass Fiber Reinforced Poly(olefin ketone) Composites, and Polyamide 6 Composite.	95

Chapter 1

Introduction

1.1. Palladium-Catalyzed Alternating Copolymerization and Terpolymerization of Alkenes and Carbon Monoxide

In the second half of this century the use of polymers in our daily life has rapidly grown in volume as well as in the number of applications. However, the chemical industry faces an ongoing maturization of the polymer business and the concurrent developments have sometimes led to the belief that the rise and decline of polymer science is already us[1].

During the last recession a number of companies have indeed reshuffled their product mix and have withdrawn themselves to core-activities[2]. Obviously the market entry-barriers for new products have increased in time, however, this should not imply that there is no room left for further improvement of the present product portfolio. In view of the high entry-barriers for mature markets, the economical feasibility of new developments is of primary concern in order to gain insight into the viability of new polymer products.

New or modified polymerization catalysts have provided the opportunity to produce new polymer materials. Some of these developments either have been commercialized or have potential to enter the highly competitive engineering or commodity plastics markets.

The development of new metallocene based catalyst systems allowed synthesis of several new resins with some exciting properties. In 1985 chemists from Idemitsu Kosan synthesized syndiotactic polystyrene (sPS) for the first time[3,4]. This process was later

expanded by Dow Chemicals Company, with developed catalysts allowing commercial production of sPS[5,6]. sPS is a semi-crystalline polymer with a relatively high glass transition temperature and a high melting point (270 °C)[7]. In addition to these good thermal properties, sPS is both chemical and water/steam resistant.

Another important development was the use of metallocene catalysts to produce syndiotactic and isotactic polypropylene (sPP and iPP). Metallocene based iPP is being commercialized by Exxon Chemical Company under the trade name EXXPOL PP[8]. This polymer has a narrow molecular weight distribution (MWD) and a narrow tacticity distribution. The formation of atactic chains is completely suppressed. During melt processing metallocene based EXXPOL PP is more easily extensible in fiber spinning than its broader MWD counterparts. The narrow tacticity distribution increases stiffness, which is useful in durable goods applications. sPP was commercialized by the Fina Oil Company[9].

The most significant improvement in the area of polyolefins was the development of constraint geometry catalysts by the Dow Chemical Company[10]. Single site metallocene based catalyst technology is known to produce homogeneous random olefin copolymers with very narrow molecular weight distribution and comonomer distribution, which together improve the physical properties. INSITE-Technology is unique among single-site catalyst technologies as it utilizes a constraint geometry catalyst, which creates long branches on narrow MWD polymers[11]. It is found that this type of structure combines excellent processing and high performance, unusual given the conventional

sacrifice of one for the other. Through INSITE-Technology, scientists at Dow Chemical have also been able to control the desired levels of long chain branches to meet customer performance and processing needs.

There has been considerable interest in aliphatic poly(ketone) (PK) polymers[12]. For example, Shell Chemical Co. produced a range of new high performance materials marketed under the tradename of “Carilon”[13-15] and BP Chemicals was introducing similar materials under the name “Ketonex”[16]. Such materials are semicrystalline and are expected to find a wide variety of applications ranging from high performance, engineering applications to barrier films.

A optimized approach to new polymer materials is the development of the group of cis-fixed palladium bidentate catalysts, which can be used for the production of alternating polyolefin ketones[17-20]. In view of the chemical structure of this class of polymers, it was anticipated that these materials can be used for engineering plastic and fiber applications [21,22].

The alternating copolymerization of ethylene and carbon monoxide has attracted considerable interest from both academia and industry[23,24] The base materials are readily available, while the product “polyketone” (poly-3-oxotrimethylene), is predicted to have interesting engineering plastic type properties, typical for polymers with a high density of heteroatom functionalities. Also, the carbonyl group can be used for derivatization to a variety of interesting new materials.

Nearly 40 years of research have evolved between the first discovery by Reppe of

metal-catalyzed alternating ethylene/CO copolymerization and the discovery at Shell of a class of highly active, high yield palladium catalysts for this reaction. These catalysts made possible the essential technological advances in the synthesis and processing of alternating polyketones which enabled Shell to move these polymers to commercial reality[25].

Nickel was the first transition metal used to catalyze the copolymerization of CO and ethylene. In the late 1940s, Reppe and Magin[26] showed that $K_2Ni(CN)_4$ in water produced low-melting oligomers of ethylene and carbon monoxide in addition to diethyl ketone and propionic acid. In the early 1970s, workers at Shell Development (Houston) succeeded[27] in improving the catalyst by the addition of strong acids such as Trifluoroacetic acids in solvents such as Methanol. They obtained a polymer with a relatively high molecular weight, but the yield of polymer per gram of catalyst was still low. After the high-yield palladium catalysts had been discovered, Klabunde[28] reported a new nickel catalyst for the alternating CO/ethylene copolymerization, based on a bidentate anionic phosphorus-oxygen ligand. Similar catalysts are also used in the Shell process for the oligomerization of ethane. Interestingly, the copolymerization has to be started with pure ethylene, even for polyketone formation. The use of SHOP-type catalysts for polyketone formation has also been claimed by Keim[29].

Palladium catalysts for alternating polyketone formation were first disclosed by Gough in 1967[30]. These catalyst systems were bis(tertiary phosphine)palladium dichloride complexes which yielded polyketone at a rate of around $300 \text{ g (g of Pd)}^{-1} \text{ h}^{-1}$. The

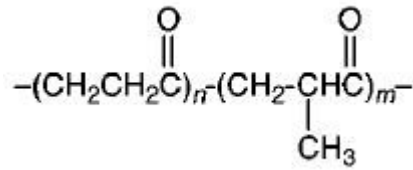
disadvantage was that severe conditions were required (250 °C, 2000 bar) and that yields in gram of polymer/gram of palladium were low. During the following 15 years, only small advances were made in increasing catalyst efficiency. Research by Shell Development Company[31] uncovered several related palladium chlorides, cyanides, and zerovalent complexes, which in a variety of solvents were also catalysts. These operated under milder conditions than those used (typically 120 °C, 70 bar), but both activities and yields were still very low. In the early 1980s, Sen and co-workers[32] published work which showed that certain tertiary phosphine-modified palladium complexes containing the weakly coordinating tetrafluoroborate anion in dichloromethane produced polyketone under very mild conditions. However, again the reaction rates ($\sim 4 \text{ g (g of Pd)}^{-1} \text{ h}^{-1}$) were very low, as were the yields (in gram of polymer/gram of palladium) and the molecular weights of the polymer.

In the early 1980s two important independent advances occurred. In 1980, workers at Shell Development Company in Houston could demonstrate melt processability of polyketone produced by palladium cyanide catalysts, after extensive extraction of catalyst residues from the polymers and blending these with other polymers such as styrene/acrylonitrile copolymer. From these studies it was suggested that thermoplastic properties were possible in principle and that the polyketone backbone was not inherently unstable in the melt as previously concluded. However, it was also clear that catalyst extraction did not offer a viable production option from a technical and economic viewpoint.

During this period, at Shell Research in Amsterdam, cationic palladium complexes containing tertiary phosphine ligands and weakly coordinating anions (e.g. sulfonates), similar to those studied by Sen, were studied in methanol as catalysts for the methoxycarbonylation of ethylene to give methyl propionate. In experiments using bidentate tertiary phosphine ligands, it was surprisingly observed that no methyl propionate product was formed; instead, high molecular weight polyketone was formed at very high rates ($\sim 6000 \text{ g (g of Pd)}^{-1} \text{ h}^{-1}$). These catalysts are very active, and yields above 10^6 have been achieved under economically attractive mild reaction conditions (90°C , 45 bar). Also, the catalysts are easy to prepare either separately or in situ[33,34]. This discovery of the combined importance of bidentate ligands and weakly coordinating anions for high catalyst activity and yield, has for the first time-opened the way for efficient synthesis of polyketone.

Equally important, these catalysts provided more stable polymers with catalyst residues now measured by parts per million rather than percent.

Chemically PKs are simply a modification of the alternating copolymer of ethylene and carbonyl units. The melting point, T_m , of the perfectly alternating copolymer of $\sim 260^\circ\text{C}$ can be lowered by incorporating a small fraction of CH_3 side groups on the chain, consequently widening the temperature window of melt processibility. The final polymer is therefore a terpolymer, the chemical structure of which may be written as (where $n/m \sim 16$).



The distribution of the CH₃ units along the chain is considered to be random[35]. The melting point falls progressively with increasing propylene content[12], reaching a value of ~220 °C at ~6 mol % of propylene. This is the concentration of CH₃ in the commercial Shell material.

1-2. Poly(1-oxotrimethylene) Fibers Prepared by Different Draw Ratios for the Tire Cord Application

Aliphatic polyketones prepared by the polymerization of carbon monoxide and olefin gases have been employed as a fiber, engineering plastic, and composite materials in many industrial fields due to their excellent tensile strength, chemical and wear resistance, good impact behavior over a broad temperature range, and very low permeability[36-43]. Various synthetic procedures used for the preparation of copolymers from ethylene and carbon monoxide gases were developed. For example copolymers with various molar ratios of ethylene and carbon monoxide were obtained using several types of peroxide initiators via γ -irradiation method[44,45]. Particularly an alternating copolymer, poly(1-oxotrimethylene), could be formed using transition metal catalysts and polymer fibers exhibiting excellent mechanical properties[36,41]. The poly(1-oxotrimethylene) fibers are normally obtained by wet spinning process and this process comprises five steps which are dissolving the polymer powder in aqueous solution with metal salts, solidifying to a cold coagulation bath, rinsing, drying, and finally drawing. Each step is of key importance since small changes in the process conditions, such as the metal salt composition, coagulation bath temperature, drying temperature, and drawing ratio, can affect the fiber properties significantly. Recently, Kato *et al.* revealed that the metal salt composition, coagulation conditions, and drying temperatures are important factors determining the structures and properties of poly(1-oxotrimethylene) fibers[46-49].

However, detailed studies on the crystal structures and mechanical properties of poly(1-oxotrimethylene) fibers with different draw ratio has not been reported in any literature yet.

Recently, the demands of tire cords having high tensile strength and modulus are gradually increasing for the applications in the high performance tires[50]. However fibers having high mechanical properties, such as rayon and aramid, have been known have poor adhesion on rubber materials, then this could limit the fabrication of high performance. Polyketone fibers have been known to have excellent adhesion, comparable with PET, nylon and aramid, and good fatigue resistance in comparison with PET and rayon[50]. Furthermore the tensile strength and modulus of polyketone fibers are higher than those of PET and nylon that as currently used for the tire cords.

Herein, we report the optimized synthetic procedure for the preparation of the poly(1-oxotrimethylene). The effect of the processing parameters such as drying temperature and draw ratio on the mechanical properties of poly(1-oxotrimethylene) investigated. Aliphatic polyketone fibers having high mechanical properties could be prepared from the optimum processing conditions. The effects of the processing conditions on the crystal structures and mechanical properties were systematically studied using differential scanning calorimetry (DSC), X-ray diffraction, and universal testing machine (UTM).

1.3. Preparation and Properties of Glass Fiber-Reinforced Poly(olefin ketone) Composites

Polyolefin ketone polymer, synthesized from carbon monoxide and olefin used as monomer, provides excellent mechanical strength, chemical resistance, abrasion resistance, gas barrier property, high fracture toughness and impact resistance, and therefore has been intensively researched due to its extensive range of applications such as fiber, engineering plastic and composites. Specifically, there is a surging demand for polyolefin ketone polymer, which outperforms the existing materials in terms of mechanical strength, rubber adhesion, and price competitiveness, etc., in the fields of rubber-reinforced fibrous composite materials, or tire code, mechanical, electric, electronic parts[36-37]. Polyolefin ketone polymer exhibits a variety of physical properties and finds extensive applications in a wide range of fields, depending on the type of olefin used as monomer. In particular, linear alternating copolymer composed of carbon monoxide and ethylene are most commonly used along with terpolymer composed of carbon monoxide, ethylene, and propylene. Researches have been variously conducted to develop the engineering process incorporating the methodologies that involve the physical properties and structure of these polymers[39,51,52].

Polymer composites can be produced by introducing the reinforcement into the polymer through simple engineering process and has excellent mechanical properties comparable to those of inorganic matters such as metal and ceramic.

Moreover, polymer composites have additional properties, such as corrosion resistance, high elasticity, etc., and therefore have found extensive applications in various fields. Among the most typical fiber-reinforced materials (fibrous reinforcement) which are introduced into those composite materials mentioned above include glass fiber, carbon fiber, aramid fiber, and others.

Specifically, glass fiber has the advantage of low cost and easiness of processability, as well as fulfill major requirements, and resultantly has been constantly used as the optimized reinforcement in universal composite materials [53-57]. Generally, the fibrous reinforcement effect of fiber-reinforced composites is mostly determined by the strength, size, dispersion of the reinforcement, and the interfacial properties between the applied reinforcement and polymer matrix is considered the most important factor. Although the polymer or reinforcement has the bonding force beyond a certain degree, their interfacial surface determines the overall uniformity of composite material which immediately affects the physical properties of composites. Thus, various surface treatment methods have been proposed to achieve the enhancement of interfacial adhesion, and the glass fiber with proper surface treatment in various polymer matrixes has been made commercially available.

In this study, the surface-treated glass fiber was introduced to develop the composite material providing the enhanced physical properties of polyolefin ketone polymer that can find application as the engineering plastic. Polyolefin ketone was synthesized from carbon dioxide, ethylene, and a small amount of propylene, and the glass fiber – treated

by urethane and amino silane or urethane and epoxy, and amino silane – was used as reinforcement. Interfacial structure analysis was carried out, using the scanning electron microscopy (SEM), to determine the compatibility of polymer matrix and glass fiber. This study was intended to examine the applicability of polyolefin ketone polymer as the engineering plastic by identifying the mechanical properties of composites based on each glass fiber.

1.4. Survey of this Thesis

To gain insight into the potential of the perfectly alternating ethylene-carbon monoxide copolymer (POK-C₂) as a starting material for industrial fibers, this polymer has been spun from aqueous solution containing a mixture of metal salts. In a subsequent drawing stage the required molecular orientation has been induced. It is well known that the mechanical properties of polymer fibers are strongly governed by the degree of molecular orientation in the direction of the fiber axis. In addition, there is a surging demand for polyolefin ketone polymer, which outperforms the existing materials in terms of mechanical strength, rubber adhesion, and price competitiveness, etc., in the fields of rubber-reinforced fibrous composite materials, or mechanical, electric, electronic parts. Polyolefin ketone terpolymer also exhibits a variety of physical properties and finds extensive applications in a wide range of fields. In Chapter 2 the polymerization of co/ter-polymer is described and the mechanism of polyketone formation is presented. In Chapter 3 the structure of POK-C₂ copolymers is described. The preparation of high-strength POK-C₂ fibers is reported, and the influence of the drawing conditions on the mechanical properties is discussed. Finally, in Chapter 4 the preparation and properties of glass fiber-reinforced Ter-Polyketone composites are reported.

1.5. References

- [1] The central theme of the 8th Rolduc Polymer Meeting (1993), May 1993, Rolduc Abbey, Kerkrade, the Netherlands, was “The Rise and Decline of High Performance Polymers in Europe”.
- [2] See, for example, 1992-1994 editions of Chemical Week.
- [3] N. Ishihara, T. Seimiya, M. Kuramoto, and M. Uoi, *Macromolecules*, 19, 2465 (1986).
- [4] Idemitsu Kosan Co., Japanese Patent 05,295,029 (Idemitsu), (1992).
- [5] R. E. Campbell and G. F. Schmidt, US-Patent 4,774,301 (Dow Chemicals), (1987).
- [6] D. R. Neithamer, J. C. Stevens, and D. R. Neithmer, European Patent 418,044 (Dow Chemicals) (1989).
- [7] Y. K. Wang, J. D. Savage, D. Yang, and S. L. Hsu, *Macromolecules*, 25 (1992) 3659.
- [8] J. J. McAlpin, *MetCon '94 Proceedings*, 1994.
- [9] M. J. Elder, J. A. Ewen, and A. Razavi, European Patent 427,696 (Fina Technology Inc.), (1989).
- [10] G. M. Knight, Y. Lais, P. N. Nickias, R. K. Rosen, G. F. Schmidt, J. C. Stevens, F. J. Timmers, D. R. Wilson, G. W. Knight, S. Lai, L. Shin-Yaw, and S. Y. Lai, European Patent 416,815 (Dow Chemical), (1989).
- [11] K. W. Swogger, *MetCon '94 Proceedings* (1994).
- [12] Garbassi, F.; Sommazzi, A. *Polym. News*, 20 (1994) 201.
- [13] E. Drent,.; Jager, W. W. *Polym. Mater. Sci. Eng.* 74 (1997) 100.

- [14] Ash, C. E.; Flood, J. E. *Polym. Mater. Sci. Eng.* 74 (1997) 110.
- [15] Ash, C. E. *Int. J. Polym. Mater.* 30 (1995) 1.
- [16] Bonner, J. G.; Powell, A. K. *Polym. Mater. Sci. Eng.* 74 (1997) 108.
- [17] E. Drent, European Patent 121,965(Shell), 1984
- [18] E. Drent, J.A.M. van Breokhoven, and M.J. Doyle, *J. Organomet.Chem.*,
417(1991)235
- [19] A. Sen, *Acc. Chem. Res.*, 26 (1993) 303
- [20] M. Barsacchi, A. Batistini, G. Consiglio, and U.W. Suter, *Macromolecules*,
25(1992)3604
- [21] E. Drent, Consulting in Hyosung R&DB Labs
- [22] J. Smook, G.J.H. Vos and H.L. Doppert, *J. Appl.Polym. Sci.*, 41(1990)105
- [23] For earlier reviews, see: Sen, A. *Adv. Polym. Sci.*,73/74(1986)125;
(b) CHEMTECH, (1986) 48; (c) *Acc. Chem. Res.* 26(1993)303.
- [24] Brubaker, M. M. U.S. Pat. 2,495,286, (1950) *Chem. Abstr.*
- [25] (a) Ash, C. E. *J. Mater. Educ.* 16(1994) 1. (b) Medema, D.; Noordam, A. *Chemisch Magazine*, March 1995.
- [26] Reppe, W.; Magin, A. U.S. Pat. 2,577,208, 1951; *Chem. Abstr.* 46(1952)6143.
- [27] Shryne, T. M.; Holler, H. V. U.S. Pat. 3,984,388, 1976; *Chem. Abstr.* 1976, 85,
178219.
- [28] (a) Klabunde, U.; Tulip, T. H.; Roe, D. C.; Ittel, S. D. *J. Organometal. Chem.* 334,
(1987)141. (b) Klabunde, U.; Ittel, S. D. *J. Mol. Catal.* 41(1987)123. (c) Klabunde,

- U. U.S. Pat. 4,698,403, 1987; Chem. Abstr. 1988, 108, 151134; U.S. Pat. 4, 716,205, 1987; Chem. Abstr. 108(1988)132485.
- [29] Driessen, B.; Green, M. J.; Keim, W. Eur. Pat. Appl. 470(1992)759 A2; Chem. Abstr. 116(1992)152623. Keim, W.; Maas, H.; Mecking, S. Z. Naturforsch., 50b,(1995)430.
- [30] Gough, A. British Pat. 1,081,304, 1967; Chem. Abstr. 67(1967)100569.
- [31] Nozaki, K. U.S. Pat. 3,689,460, 1972; Chem. Abstr. 77(1972) 152860; U.S. Pat. 3,694,412, 1972; Chem. Abstr. 77(1972) 165324; U.S. Pat. 3,835,123, 1974; Chem. Abstr. 83(1975)132273.
- [32] Sen, A.; Ta-Wang Lai, J. Am. Chem. Soc. 104(1982) 3520; Organometallics 3(1984) 866.
- [33] Drent, E. Eur. Pat. Appl. 121,965 A2, 1984; Chem. Abstr. 102(1985) 46423.
- [34] Drent, E.; Van Broekhoven, J. A. M.; Doyle, M. J. J. Organomet. Chem. 417(1991)235.
- [35] Bronco, S.; Consiglio, G.; Gindro, E. L. P. Polym. Mater. Sci. Eng. 74(1997) 106.
- [36] E. Drent, and P. H. M. Budzelaar, Chem. Rev., 96(1996) 663.
- [37] B. J. Lommerts, E. A. Klop, and J. Aerts, J. Polym. Sci. B Polym. Phys., 31(1993) 1319.
- [38] E. A. Klop, B. J. Lommerts, J. Veurink, J. Aerts, and R. R. Van Puijenbroek, J. Polym. Sci. B Polym. Phys., 33(1995)315.
- [39] A. J. Waddon, N. R. Karttunen, and A. J. Lesser, Macromolecules, 32(1999)423.
- [40] J. M. Largaron, M. E. Vickers, A. K. Powell, and N. S. Davidson, Polymer, 41(2000)

3011.

- [41] E. Drent, and W. W. Jager, *Polym. Mater. Sci. Eng.*, 74(1997)100.
- [42] C. E. Ash, and J. E. Flood, *Polym. Mater. Sci. Eng.*, 74(1997)110
- [43] J. G. Bonner, and A. K. Powell, *Polym. Mater. Sci. Eng.*, 74(1997)108.
- [44] M. M. Brubaker, D. D. Coffman, and H. H. Hoehn, *J. Am. Chem. Soc.*,
74(1952)1509.
- [45] Y. Chatani, T. Takizawa, S. Murahashi, Y. Sakata, and Y. Nishimura, *J. Polym. Sci.*,
55(1961) 811.
- [46] T. Morita, R. Taniguchi, T. Matsuo, and J. Kato, *J. Appl. Polym. Sci.*, 92(2004)1183.
- [47] T. Morita, R. Taniguchi, and J. Kato, *J. Appl. Polym. Sci.*, 94(2004)446.
- [48] T. Morita, M. Adachi, and J. Kato, *J. Appl. Polym. Sci.*, 96(2005)1250.
- [49] T. Morita, and J. Kato, *J. Appl. Polym. Sci.*, 100(2006) 3358.
- [50] Y. Zuigyo, *Tire Sci. and Technol.*, 35(2007)317.
- [51] A. J. Waddon, and N. R. Karttunen, *Macromolecules*, 35 (2002)4003.
- [52] T. Morita, R. Taniguchi, T. Matsuo, and J. Kato, *J. Appl. Polym. Sci.*, 92(2004)1183.
- [53] P. K. Mallick, *Fiber-reinforced Composites*, Marcel Dekker, New York, (1988).
- [54] J. W. Cho, and D. R. Paul, *Polymer*, 42(2001)1083.
- [55] J. S. Jang, *J. Korean Ind. Eng. Chem.*, (1990)133.
- [56] S.-J. Park, J.-X. Jin, and J.-R. Lee, *J. Korean Ind. Eng. Chem.*, 12(2001)143.
- [57] K. Na, H. S. Park, and H. Y. Won, *Macromol. Res.*, 14(2006)499.

Chapter 2

Palladium-Catalyzed Alternating Copolymerization and Terpolymerization of Alkenes and Carbon Monoxide

2.1. Introduction

This description presents the process description for a 1,000ton/yr polyketone polymer plant to be located at Ulsan, Korea. The design and experiment are based on batch slurry process technology developed by Hyosung from studies conducted at the R&DB Center and pilot plant. The plant design presented has two batch reactors and agitator. All other equipment and plant design were for a first time constructed polyketone plant, i.e. in Korea, there is nothing else to copy from the Shell Patents. Originally, polyketone is the alternating copolymer of carbon monoxide and olefin monomer units. The copolymer itself has been known for over 40 years. The terpolymers are trimmers in that they contain 6wt% propylene in addition to the ethylene and carbon monoxide, and polymerization process were optimized recently. The reaction parameters of polyketone polymerization were well known by Shell Oil Company, BP, and Hyosung, so it is not suitable to describe them in detail in this section. Therefore, The mechanism of polymerization is described briefly and the effect of reaction temperature and time on LVN, Molecular weight, and Bulk Density(BD) is reported and the direct correlation between LVN and Melting Index(MI) is also described. The chemical and physical properties of the polymers were characterized with Ostwalds viscometer, Gel Permeation Chromatography(GPC), and Scanning Electron Microscopy (SEM).

2.2. Experimental

The copolymer is made by polymerizing ethylene and carbon monoxide in a 50% mass/molar ratio. The CO:Olefin molar ration in both products is 1:1. The polymer grades are characterized by their melting point and Limiting Viscosity Number(LVN). The copolymer has a higher melting point(260°C) than terpolymer. At about 252°C the polymer has the undesirable effect of cross-linking. The small temperature difference between the polymer melting and cross-linking temperature makes it difficult to process without product degradation. The technology for extruding this grade of polymer, without excessive cross linking, is still under development. The addition of propylene to make the terpolymer lowers the melting point, such that, with the proper additive package it can be extruded without cross-linking. The LVN of the final polymer is a function of the reaction pressure, temperature, and monomer concentrations. However, during polymerization, only the temperature is varied to control the LVN. The other variables are held constant. The design is based on only two grades of terproduct, R1000 and P1000. Both have a melting point of 220°C. P1000 has a LVN of 1.8 while the LVN for R1000 is 1.1.

Polymerization Chemistry

The polymerization reactions are carried out in batch reactors at 725-800 psig(51~56kg/cm²g) and 76.7~87.8°C in the presence of a palladium catalyst complex. As the polymer is produced, it forms a slurry in the methanol solvent. A small portion of

the solvent reacts with the polymer. The reactions are as follows:

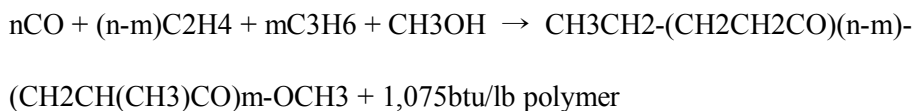
Copolymer



For LVN = 1, n=270

For LVN = 2, n=650

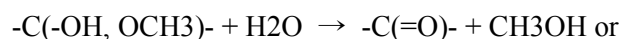
Terpolymer



For polymer Grade P1000, LVN=1.8 with n=648, m=53

For polymer Grade R1000, LVN=1.1 with n=272, m=22

Water is required as an additive to the reactor system to control the formation of “ketals” by reaction of the methanol solvent with the carbonyl groups in the polymer backbone.

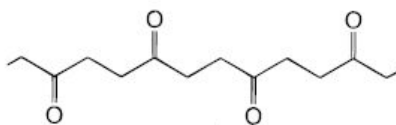


Trace amounts of metal ions have deleterious effects on the polymerization rates and, most importantly, on the product melt stability. Particularly troublesome ions include sodium, potassium, iron and amines. The research into the limits and importance of the

ionic contamination of the solvent and polymer is ongoing. The iron content of the methanol should be less than 1ppmw.

Polymerization Mechanism[1]

The copolymerization is catalyzed by a palladium(II) diphosphine complex with weakly or non-coordinating anions. Depending on the choice of ligand and process conditions, rates can be very high, and molecular weights can be varied over a wide range [2,3].



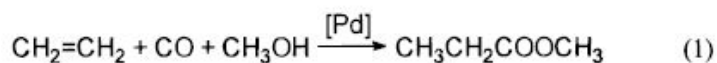
Palladium catalysts for alternating polyketone formation were first disclosed by Gough at ICI in 1967 [4]. This catalyst system, the disadvantage was that severe conditions were required and that yields in gram of polymer/gram of palladium were low.

Two important advances occurred independently at the beginning of the 1980s. In 1982 Sen and co-workers published work which showed that certain tertiary phosphine-modified palladium complexes containing the weakly coordinating tetrafluoroborate anion in dichloromethane produced polyketone under very mild conditions-in glass at room temperature. The reaction rates were low (4g/g Pd/hr) but the reported melting point of the product (260°C) indicated the molecular weight to be high [5].

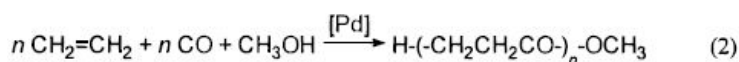
During this period, at Shell Research, cationic palladium tertiary phosphine complexes

in methanol were studied as catalysts using bidentate phosphine ligands, It were surprised to find no methyl propionate product; instead, high molecular weight polyketone was formed at very high rates (~6000g/g Pd/hr). These catalysts are very powerful, and turnovers in the order of 10^6 have been achieved under economically attractive mild reaction conditions (90°C, 45bar). Also, the catalysts are easy to prepare either separately or in situ [3,6,7].

The discovery of efficient catalysts for the copolymerization of CO with olefins originated from a study of the alkoxy carbonylation of ethylene to methyl propionate (eq 1).

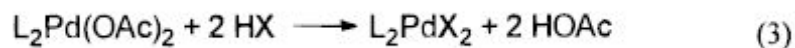


The catalysts were cationic palladium phosphine systems prepared from palladium acetate, an excess of triphenyl phosphine(PPh₃), and a Brønsted acid of a weakly or noncoordinating anion, methanol was used both as a solvent and a reactant. A surprising and remarkable change in selectivity was observed upon replacement of the excess of PPh₃ by a stoichiometric amount of the bidentate ligand 1,3-bis(diphenylphosphino)propane (dppp). Under the same conditions, these modified catalysts led to the production of a perfectly alternating CO/ethylene copolymer with essentially 100% selectivity (eq 2) [3,6,8].



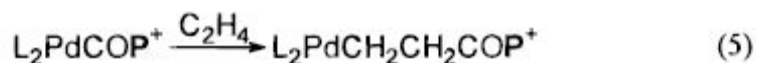
A typical reaction rate would be 10^4 mol of converted ethane/molPd/hr, to give a

polymer with an average molecular weight(M_n) of 20,000(dppp/HOTs/MeOH, 65°C) [6]. Under suitable conditions, the catalysts are highly stable and total conversions of more than 10^6 mol of ethylene per mole of Pd can be obtained. The product has a high melting point (260 °C) and is insoluble in most organic solvents (the most important exception being HFIPA); it precipitates during copolymerization as a snow-white solid. Variation of the bidentate ligand results in significant changes in both the reaction rate and the molecular weight of the product. The anions can conveniently be introduced by adding a Brønsted or Lewis acid as the anion source to the palladium acetate.



Propagation

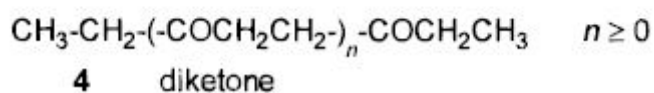
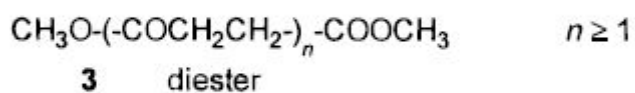
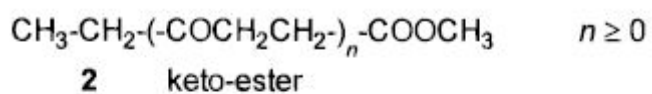
The catalytically active species in polyketone formation is thought to be a d^8 square-planar cationic palladium complex L_2PdP^+ (L_2 : represents the bidentate ligand, P: the growing polymer chain). The fourth coordination site at palladium may be filled by an anion, a solvent molecule, a carbonyl group of the chain, or a monomer molecule. Thus, the two alternating propagation steps are migratory insertion of CO into the palladium-alkyl (eq. 4) bond and migratory insertion of ethylene into the resulting palladium-acyl bond (eq. 5).



Carbon monoxide insertion in a palladium-carbon bond is a fairly common reaction [9]. Under polymerization conditions, CO insertion is thought to be rapid and reversible. Olefin insertion in palladium carbon bonds is not as common.

Initiation and Termination

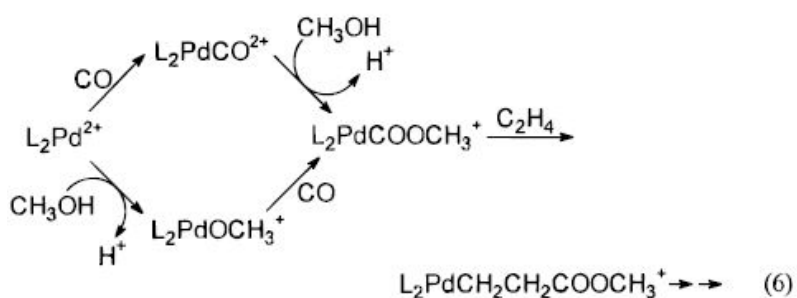
End group of the CO/ethylene copolymer has demonstrated the presence of 50% ester (-COOCH₃) and 50% ketone (-COCH₂CH₃) groups, in accord with the average overall structure of the polymer molecule as given above in eq 2. Moreover, GC and MS presence of diester(3) and diketone(4) compounds [6].



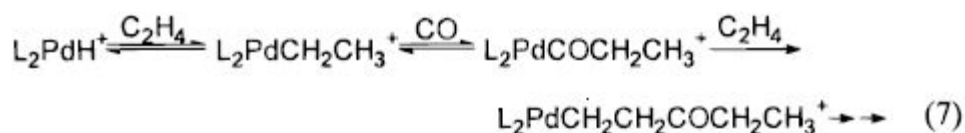
At low temperatures (≤ 85 °C), the majority of the products are keto esters, with only small, but balancing, quantities of diesters and diketones. At higher temperatures, the same products are produced in a ratio (2:3:4) close to 2:1:1. These observations have been

explained [6] by assuming two initiation and two termination mechanisms for polyketone formation.

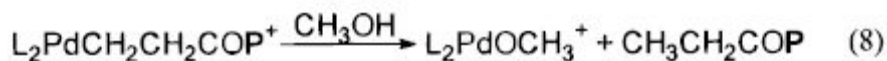
One initiation path way produces ester end groups. It starts with a palladium carbomethoxy species [6,10], which can be formed either by CO insertion in a palladium methoxide or by direct attack of methanol on coordinated CO (eq 6).



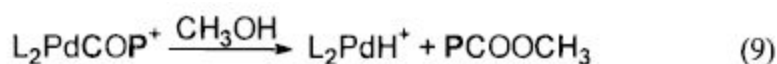
Alternatively, a chain can start by insertion of ethylene in a palladium hydride [5,6], producing a ketone end group. Ethylene insertion in a palladium hydride and CO insertion in the resulting ethyl complex are both rapid and reversible; it is thought that the second ethylene insertion (in the Pdacyl) is irreversible and “traps” the acyl to start the chain (eq 7).



For CO/ethylene copolymerization, two relevant termination mechanisms have been proposed. One mechanism, protolysis of the palladium-alkyl bond, produces a saturated ketone end group (eq 8).



A second mechanism, the alcoholysis of the palladium-acyl bond, gives an ester end group (eq 9).



Catalyst Chemistry

The catalyst complex is formed from a palladium salt, phosphine ligand and an organic acid. It is produced as a solution in acetone. The palladium compound(PC) is palladium acetate. In the polymerization reaction, the catalyst concentration is based on the Pd to polymer ratio; 20ppmw Pd on polymer. Half of the palladium remains on the product.

The Ligand compound(LC) of choice for this design is BDOMPP or 1,3 bis(di-orthomethoxyphenylphosphino)propane.. The theoretical molar ratio of palladium to ligand is 1:1. Insufficient ligand can lead to plating out of metallic palladium. An excess of ligand reduces the catalyst activity. Experiments are based on a five percent excess partly to make up for some inert, soluble Pd compounds formed with impurities present with the ligand. If a higher purity ligand becomes available, it may become possible to lower the ration to the theoretical optimum value of 1.0.

The organic acid for this experiments is trifluoroacetic acid(TFA). Like the ligand, other acids are in development but no changes in the experiments. The acid:palladium molar ratio can vary between 2:1 and 20:1, depending on the product grade being

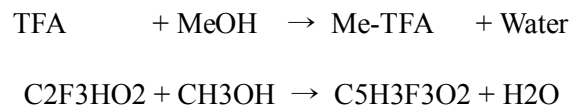
produced and the operating requirements. A minimum ration of 2:1 acid is always added as part of the catalyst system. The design case is for a ratio of 6:1 for P1000 and 10:1 for R1000.

The catalyst is formed in a batch reactor at ambient temperature and pressure. The LC is first dissolved in acetone(2-hours). The PC is then added and allowed time to react(2hours). TFA is then charged to the reactor. The reactions are as follows:

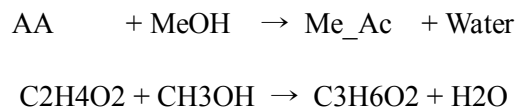


Once the catalyst is added to the polymerization reactor, there are side reactions that take place with the methanol solvent.

- (1) The excess TFA slowly esterifies forming methyl-trifluoroacetate at an equilibrium concentration.

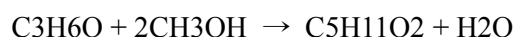


- (2) It is assumed that all of the acetic acid reacts to form methyl acetate.



- (3) It is assumed that 50% of the acetone is converted to 2,2-dimethoxypropane.





Process outline

The catalyst is produced on site in a batch reactor. The polymerization is carried out in two batch reactors. After polymerization is complete, the batch is gravity drained to a shared Monomer Recovery Vessel. The Monomer Recovery Vessel is then isolated from the reactor and the reactor is charged with seed slurry. A two-stage Monomer Recovery Compressor pumps most of the excess monomers from the Monomer Recovery Vessel back to the reactor. At the same time, methanol and the initial monomer charges are added to the reactor. After the monomer is recovered and the monomer concentrations and reactor temperature are established, the batch is initiated by catalyst addition.

After the Monomer Recovery Vessel has been depressurized, by Monomer Recovery Compressor, its contents are gravity drained to the Slurry Surge Vessel. This vessel provides the surge capacity to go from the batch reactors to a continuous process for recovering the solvent, drying the polymer powder, adding additives and extrusion into pellets or nibs. The continuous process consists of a centrifuge, 2-stage powder drying system, powder surge, additive addition, additive blending, extrusion, and .

Process chemicals

Ethylene and Propylene Monomers

Ethylene and Propylene are supplied by pipeline from Hyosung at pressures above

maximum process requirements. The only treatment of these streams are guard filter to remove rust contamination.

Carbon Monoxide Monomers

Carbon Monoxide are supplied by tube trailer(100 bar) from AirLiquide Korea.

Process Solvent

Methanol is the process solvent. It is delivered to the plant by tank truck. All incoming methanol is mixed with process contaminated methanol in the Used MeOH Storage Tank. That is, most of the contaminated solvent returning from the process will bypass the tank and go directly to the methanol recovery column. The new methanol from tank trucks is passed through the column before use to remove iron and unknowns. Operation of the

Purified methanol from the methanol recovery column is stored in the Clean Methanol Tank.

Acetone

Acetone is the solvent used for catalyst manufacture. It is received by truck from Samsung and stored in the Acetone Storage Tank.

Deionized water

Deionized water will be supplied from common facilities. There are two continuous process uses of deionized water. The biggest consumer will be for the pelletizer(6-8gpm). Water is also added to the polymerization reactor via methanol addition(1-2 gpm of water are added to the methanol product as it exits from the Methanol Recovery Column).

Catalyst Preparation

The catalyst production process takes place at ambient conditions and produces no heat or pressure. The reaction can take place anywhere between 0 °C and 35°C.

Acetone is first charged to the catalyst reactor. The LC is dumped into the reactor. After a period of time is allowed to dissolve the LC, the PC is charged to the reactor. This results in a catalyst system with a Pd concentration of 1 gram/liter of acetone. After the TFA is allowed to react. This completes the steps required to make the catalyst complex. Metering accuracy of all components but TFA should be within 0.5wt%. TFA may be plus or minus 5%.

When the reaction is complete, the batch is dropped to the Catalyst Surge Vessel. From there it is pumped to the polymerization reactors on demand. The catalyst preparation is not sensitive to oxygen, but the detail experiments should minimized oxygen addition to the polymerization reactor.

The catalyst recipe for the P1000 and R1000 products vary only by the TFA/Pd mole ratio. For P1000 the ratio is 6:1 and for R1000 the ratio is 10:1.

Polymerization

Polymerization is carried out in two stirred, semi-batch reactors operating in a carousel mode. At any point in time, one reactors are in the polymerization phase and the other reactor is being emptied and recharged. To initiate a batch, seed polymer slurry(11-14% of gross polymer in a batch) from a previous batch is pumped back from the Monomer

Recovery Vessel. The reactor is charged with methanol containing 2% deionized water and recovered monomers. The reactor is subsequently “conditioned” with respect to temperature and gas cap composition by charging ethylene, propylene and carbon monoxide and heating the reactor contents. Heat up to reaction temperature is accomplished by heating the methanol as it is charged to the reactor and by circulating vapors in the reactor gas cap through the Loop Gas Heater. Once the initial reaction conditions are set, the reaction is started by injecting catalyst. The monomer partial pressure controllers will start continuous feed of carbon monoxide and ethylene on demand.

The process requires the presence of seed polymer to achieve higher powder bulk density and to minimize reactor fouling. Reactor fouling is further suppressed by electro-polishing the reactor and its internals.

Water is added to the methanol to reduce the chemically bound methanol (formation for ketals) on the polymer.

The reaction takes place in three stages identified as Stage1, Stage2 and Starvation. Stage1 is conducted at the initial reaction temperature. After a fixed quantity of carbon monoxide has been reacted, Stage2 is initiated by increasing the reaction temperature while keeping the composition constant. Again after a fixed mass of CO has reacted, the Starvation step is initiated by stopping the addition of CO and Ethylene. This step is completed when the CO partial pressure drops to a predetermined level. The propylene concentration does not decrease much during the reaction. The reaction parameters and

them of product Specifics are listed in Table1 and Table 2.

The polymerization reaction is exothermic. A centrifugal compressor is provided to circulate vapor cap gases through a partial condenser to remove this heat. A heater is also provided to heat the reactor contents after a shutdown or to adjust the initial reactor temperature if needed.

After completion of the starvation step, the reactor is at a pressure of 39bars. The reactor is equalized with the Monomer Recovery Vessel to a final pressure 22bars. The bottom valve on the vessel is opened and the contents of the reactor are drained to the Monomer Recovery Vessel. Once the reactor is empty and the bottom and equalization valves are closed, it is ready to begin the next batch cycle.

Reactor control

Two analyzers measure the gas cap composition. The concentration of carbon monoxide is measured continuously by an infrared analyzer. A GC measures the concentration of ethylene, propylene and other components present in the gas cap.

With the total pressure measured, the individual monomer pressures are calculated and used for control. Loss of monomers during the reaction time would result in a short batch of product.

Monomer recovery

The plant was designed to recover most of the propylene, ethylene and carbon

monoxide dissolved in the slurry discharged from the polymerization reactor to the Monomer Recovery Vessel.

If the powder bulk density drops from the normal 15.6-21.8lb/ft³ to 12.5lb/ft³, as it has at the Hyosung R&DB Labs in Anyang, Korea, then the reactor sets up or experiences what has been termed a “stagnation” condition. The condition is characterized by a lost in power draw by the mixer and high temperature differentials between the thermocouples in the liquid phase. The problem is corrected by adding methanol to the reactor. To prevent stagnation in the Monomer Recovery Vessel, it is necessary to add methanol to the vessel before the reactor slurry is dropped into it. It prevents obtaining a non-Newtonian slurry as the monomers flash off.

The vapor caps between the reactor and Monomer Recovery Vessel are first equalized and then the slurry contents of the reactor are dropped, and the Seed Slurry Pump is turned on and seed for the next batch is pumped to the reactor. Next the Monomer Recovery Compressor is brought on line with the suction taken from the Monomer Recovery Vessel and the discharge going back to the reactor.

Solvent removal

The purpose of this process is to transform the ~30%wt polymer slurry into two streams; a polymer stream containing a maximum of 500ppmw methanol and a second stream of contaminated methanol that free of solids. A centrifuge and two-stage dryer systems are used to accomplish the drying. The centrifuge and dryer operate at a positive,

near atmospheric, pressure.

The slurry is pumped from the Slurry Surge Vessel to a cone type centrifuge. The cake discharged from the centrifuge is 40% liquid on a wet basis. Facilities are provided to wash the cake on the solids discharge beach of the centrifuge to lower the Pd content in the final product if desired.

The cake drops into a first-stage dryer, a horizontal, rotor and paddle type with a steam jacket. The product will exit the dryer at 110°C with a methanol concentration less than 1.0%. The “dry” polymer drops into the 2nd-stage dryer.

Powder exposure to high temperatures and oxygen must be limited.

The 2nd-stage dryer is also a rotor and paddle type dryer that provides up to 45-minutes residence time for removing the methanol content that is limited by diffusion rates. This vessel will have a once through nitrogen purge that will go to the flare. The 2nd-stage dryer will reduce the powder methanol content to 500ppmw and cool the powder to 85°C prior dropping it into a closed nitrogen conveying loop that transports it to the downstream Powder Storage Hopper. The brief flow diagram of polymerization process is represented in Figure 1.

2.3. Results and Discussion

The reaction parameters of polyketone polymerization are well known by Shell Oil Company, BP, and Hyosung, so it is not suitable to describe them in detail in this section. Therefore, The effect of reaction temperature and time on LVN, Molecular weight, and Bulk Density(BD) is reported and the direct correlation between LVN and Melting Index(MI) is also described. The LVN of the final polymer is a function of the reaction pressure, temperature, and monomer concentrations. However, during polymerization, only the temperature is varied to control the LVN. The effect of reaction temperature on the LVN is studied for one seeding powder. The runs were terminated after about 6 hours. The results are represented in Figure 2. Increasing the temperature by 8°C resulted in a reduction of LVN from 2.4dl/g to 1.3dl/g at the multi-stage reaction.

In Figure 3, the GPC data is plotted as function of the reaction temperature, and Figure 4 shows the scanning electron microscopy (SEM) images of the influence of the reaction temperature to particle size. There seems to be a strong correlation between molecular weight and reaction temperature in the both Figure 2 and Figure3. The molecular weight and LVN are decreased by increasing the reaction temperature. It can be inferred that the formation of new nuclei than growth of molecular chain is predominant, and it can be missed the chance of chain growth by increasing the reaction temperature. Those results can be correlated with the results of Figure 4. The particle size is decreased by increasing the reaction temperature. Therefore, to gain the particle with big size and high

molecular weight, the reaction temperature will optimized at lower reaction temperature.

The effect of reaction temperature on bulk density(BD) was studied for on seeding powder. Figure 5 shows that increasing the temperature by 8 °C from 81 °C to 89 °C resulted in a reduction of BD from 81 °C to 86 °C, but BD is slightly increased from 86 °C. The BD can be increased by starting the batch reaction at a lower temperature and increasing the temperature during the run. The particles with “plate-shaped” feature were formed at a lower temperature, and then the particles with “cauliflower-shaped” feature which has a lot of pores were formed by increasing reaction temperature. It can be predicted that the small particles with “plate-shaped” feature without pores was agglomerated, and changed into the “cauliflower-shaped” feature with a lot of pores. Therefore, increasing the temperature by 8 °C from 81 °C to 86 °C resulted in a reduction of BD due to the formation of particles with pores. However, the particles with pores became denser after 86 °C and BD is increased again. Those results can be directly correlated with SEM images in Figure 4. The effect of melting index(MI) on LVN was shows in Figure 6. The results can be easily predicted that the increasing the LVN resulted in a increasing of MI due to the molecular weight.

2.4. Conclusions

Polyketone terpolymers were synthesized in Hyosung. The effects of increasing the temperature resulted in a reduction of LVN, molecular weight, and particle size. In the view point of BD and feature, the particles with “plate-shaped” feature were formed at a lower temperature, and then the particles with “cauliflower-shaped” feature which has a lot of pores were formed by increasing reaction temperature. It can be predicted that the small particles with “plate-shaped” feature without pores was agglomerated, and changed into the “cauliflower-shaped” feature with a lot of pores. Therefore, increasing the temperature by 8 °C from 81 °C to 86 °C resulted in a reduction of BD due to the formation of particles with pores. However, the particles with pores became denser after 86°C and BD is increased again.

Table 2-1. Reaction Parameter of Polyketone polymerization

The following reaction parameters	bar	45
Total Inerts	%mol	5-10
Normal Operating Pressure	bar	50-55
Starvation-CO Partial Pressure	bar	6
Pd Intake On Polymer Produced	ppmw	20
Pd Residue On Final Product	ppmw	10
$C2=/(C2= + CO)$	Mol/mol	0.60
$C3=/(C2=)$ (at start)	Mol/mol	0.70
$CO/(C2= + C3=)$ (at start)	Mol/mol	0.40

Table 2-2. The reaction parameters of Polyketone product specific.

Product Specific Parameters	Units	P1000	R1000
Average Catalyst Activity	Kg Poly/Kg Pd/hr	7800	10800
Final Slurry Concentration	%	32	27
Stage1 Temperature	°C	75	82
Stage2 Temperature	°C	80	88
Stage1 CO Addition	Kg	105.78	42.31
Total CO Addition	Kg	233.59	178.54
Total Reaction Time	Hrs	6.4	4.6

Figure 2-1. The Flow Diagram of polymerization process

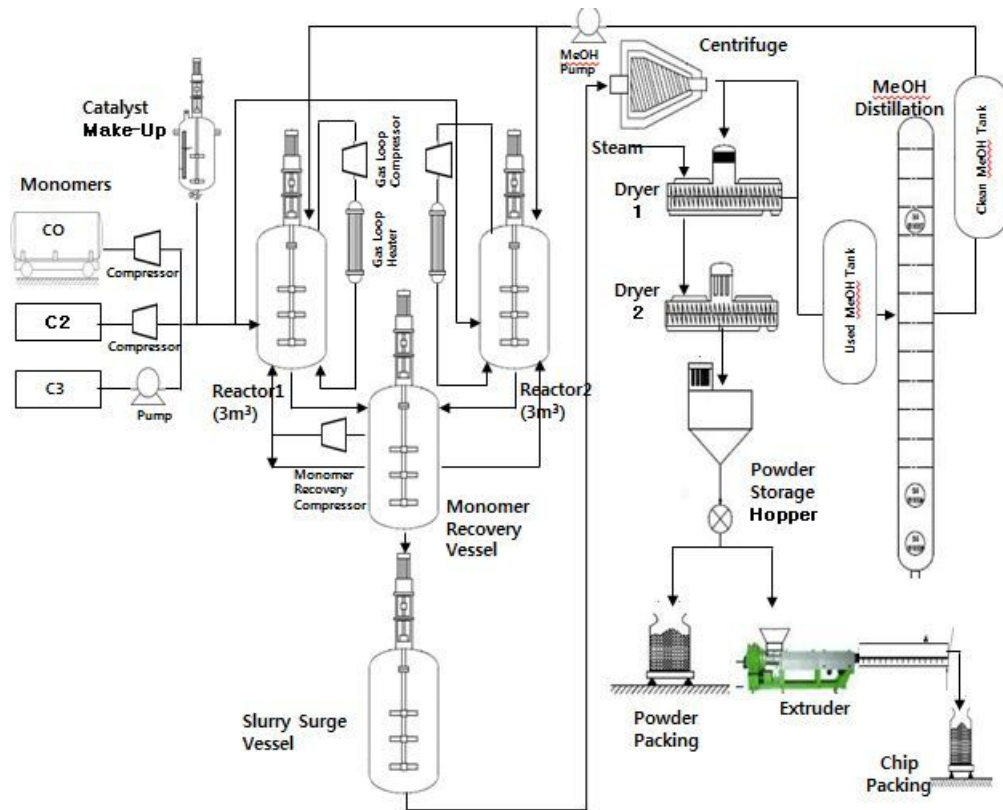


Figure 2-2. The LVN as a function of the reaction temperature

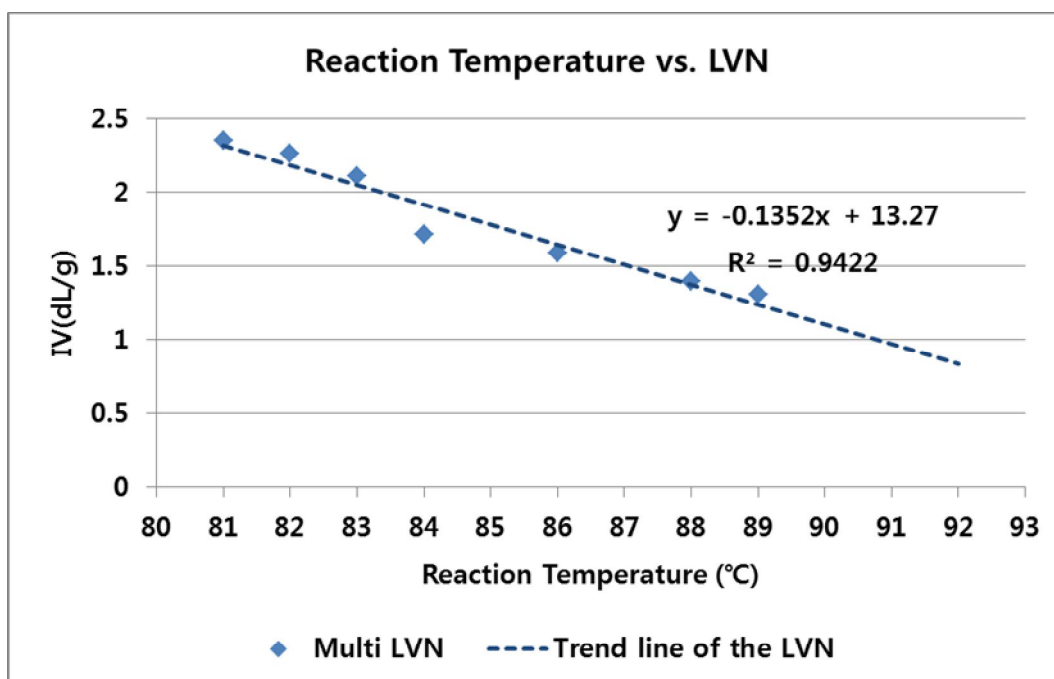


Figure 2-3. The Molecular Weight as a function of the reaction temperature

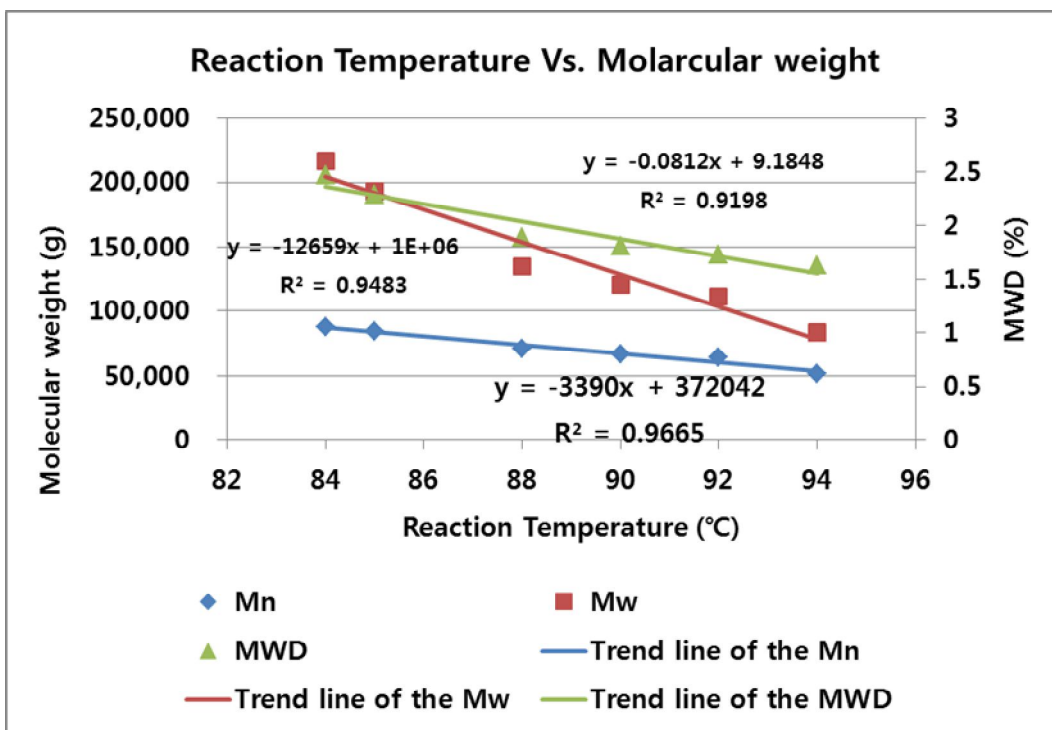


Figure 2-4. The scanning electron microscopy (SEM) images of the influence of the reaction temperature to particle size

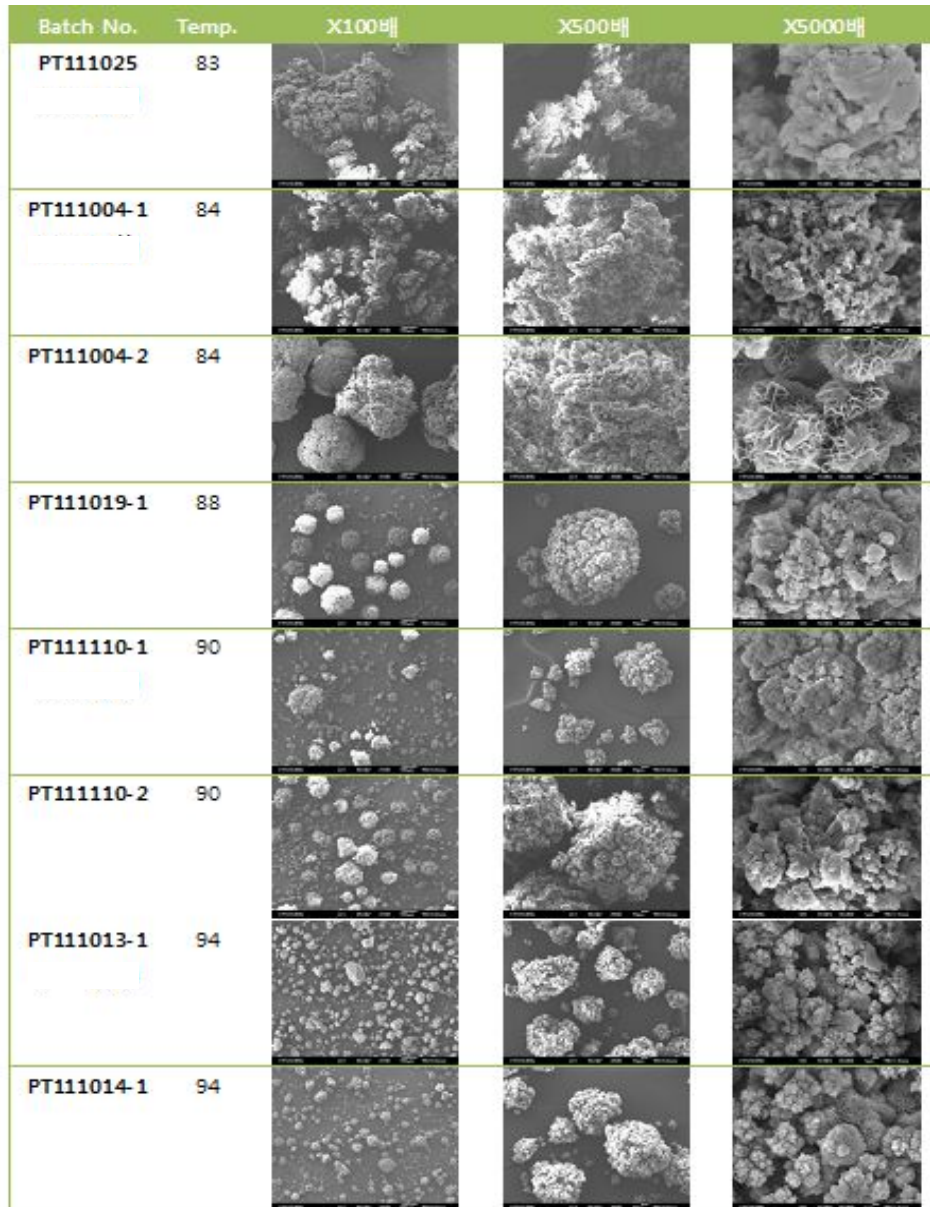


Figure 2-5. The Bulk Density(BD) as a function of the reaction temperature

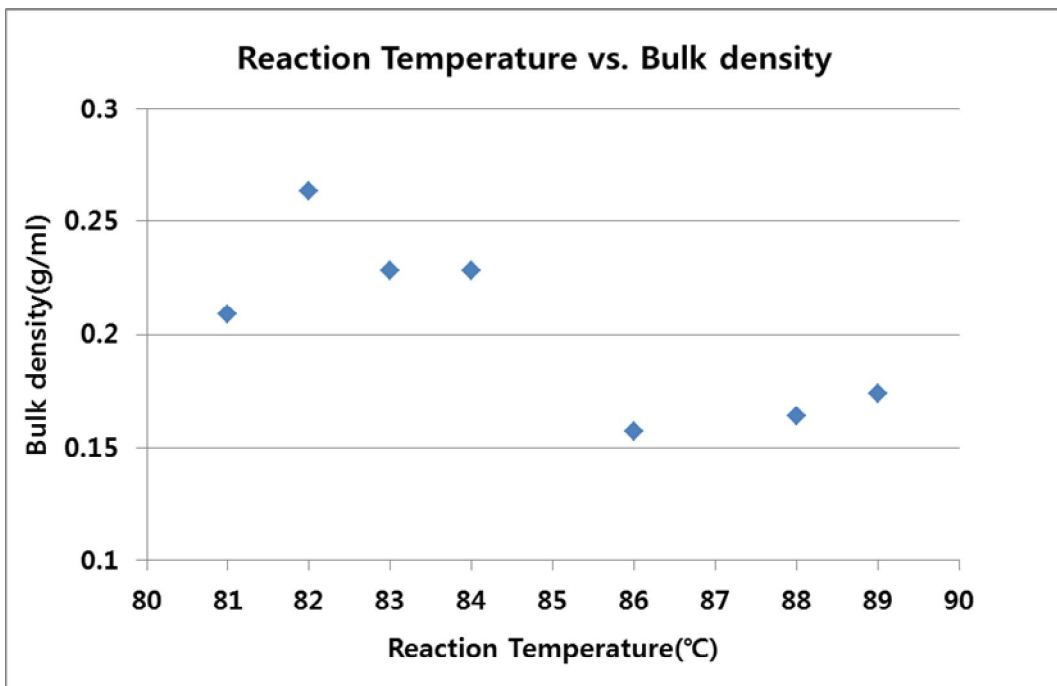
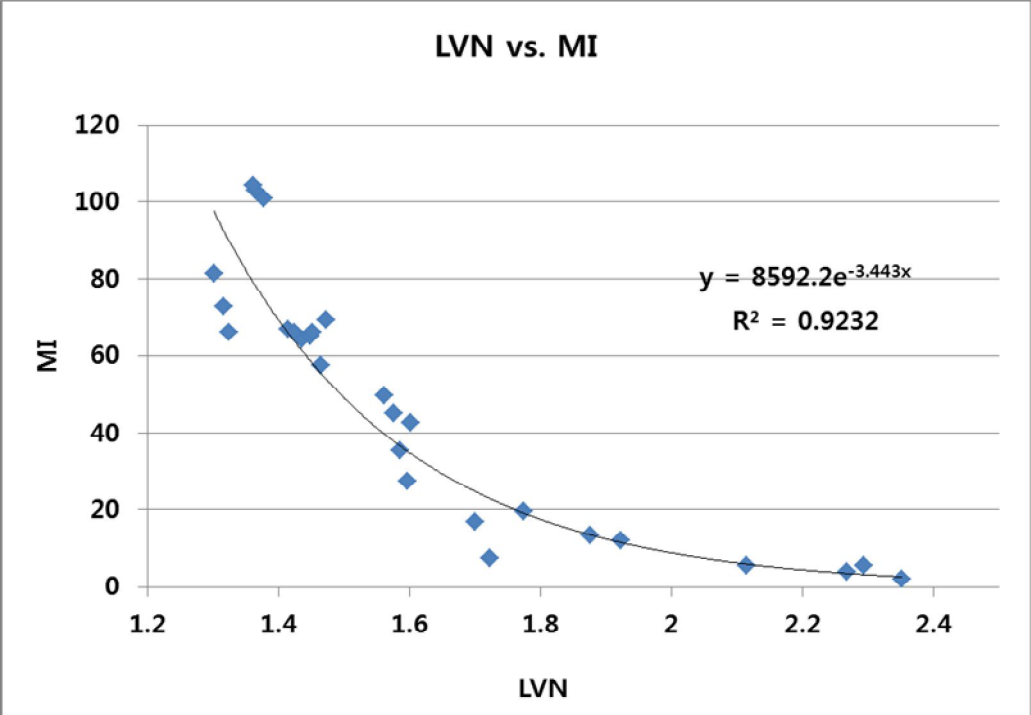


Figure 2-6. The effect of melting index(MI) on LVN



2.5. References

- [1] E.Drent and P.Budzelaar, Chem. Rev. 96(1996) 663
- [2] W. Reppe and A. Magin, U.S. Pat. 2,577,208, 1951; Chem. Abstr. 46(1952) 6143.
- [3] E. Drent, Eur. Pat. Appl. 121,965 A2, 1984; Chem. Abstr. 102(1985) 46423.
- [4] Gough, A. British Pat. 1,081(1967)304,; Chem. Abstr. 67(1967)100569
- [5] Sen, A.; Ta-Wang Lai, J. Am. Chem. Soc. 1982, 104, 3520 and Organometallics, 3(1984)866.
- [6] Drent, E; Van Broekhoven, J.A.M.; Doyle, M. J. J. Organomet. Chem. 417(1991)235.
- [7] While many catalytic reactions require considerable skill and experience, the white powder always obtained as a result of this reaction is very rewarding for the experimentalist. The reaction does not seem to be very sensitive to varying amounts of water or oxygen.
- [8] ^{13}C NMR (9/1 HFIPA/ C_6D_6 , 250MHz): d_{CO} 212.9, d_{CH_2} 35.6(1:2). Some smaller peaks due to end-groups can also be identified: $-\text{COCH}_2\text{CH}_3$, d_{CO} 217.1, d_{CH_3} 6.5; $-\text{COOCH}_3$, d_{CO} 176.5, d_{OCH_3} 52.0. The ratio of ester to ketone end-groups is generally close to 1.
- [9] See. e.g. Maitlis, P.M. "The organic chemistry of palladium", Academic Press, London, 1971. Chaloner, P. A. "Handbook of coordination catalysis in organic chemistry", Butterworths, London, 1986. Yamamoto, A. "Organotransition metal chemistry", Wiley, New York, 1986.
- [10] Jiang, Z.; Dahlen, G.M.; Houseknecht, K.; Sen, A. Macromolecules 25(1992)2999.

Chapter 3

Poly(1-oxotrimethylene) Fibers Prepared by Different Draw Ratios for the Tire Cord Application

3.1. Introduction

Aliphatic polyketones prepared by the polymerization of carbon monoxide and olefin gases have been employed as a fiber, engineering plastic, and composite materials in many industrial fields due to their excellent tensile strength, chemical and wear resistance, good impact behavior over a broad temperature range, and very low permeability [1-8]. Various synthetic procedures used for the preparation of copolymers from ethylene and carbon monoxide gases were developed. For example copolymers with various molar ratios of ethylene and carbon monoxide were obtained using several types of peroxide initiators via γ -irradiation method[9,10]. Particularly an alternating copolymer, poly(1-oxotrimethylene), could be formed using transition metal catalysts and polymer fibers exhibiting excellent mechanical properties[1,6]. The poly(1-oxotrimethylene) fibers are normally obtained by wet spinning process and this process comprises five steps which are dissolving the polymer powder in aqueous solution with metal salts, solidifying to a cold coagulation bath, rinsing, drying, and finally drawing. Each step is of key importance since small changes in the process conditions, such as the metal salt composition, coagulation bath temperature, drying temperature, and drawing ratio, can affect the fiber properties significantly. Recently, Kato *et al.* revealed that the metal salt composition, coagulation conditions, and drying temperatures are important factors determining the structures and properties of poly(1-oxotrimethylene) fibers[11-14]. However, detailed studies on the crystal structures and mechanical properties of poly(1-

oxotrimethylene) fibers with different draw ratio has not been reported in any literature yet.

Recently, the demands of tire cords having high tensile strength and modulus are gradually increasing for the applications in the high performance tires[15]. However fibers having high mechanical properties, such as rayon and aramid, have been known have poor adhesion on rubber materials, then this could limit the fabrication of high performance. Polyketone fibers have been known to have excellent adhesion, comparable with PET, nylon and aramid, and good fatigue resistance in comparison with PET and rayon[15]. Furthermore the tensile strength and modulus of polyketone fibers are higher than those of PET and nylon that as currently used for the tire cords.

Herein, we report the optimized synthetic procedure for the preparation of the poly(1-oxotrimethylene). The effect of the processing parameters such as drying temperature and draw ratio on the mechanical properties of poly(1-oxotrimethylene) investigated.

Aliphatic polyketone fibers having high mechanical properties could be prepared from the optimum processing conditions. The effects of the processing conditions on the crystal structures and mechanical properties were systematically studied using differential scanning calorimetry (DSC), X-ray diffraction, and universal testing machine (UTM).

3.2 Experimental

Materials

1,3-Bis[di(2-methoxyphenyl)phosphino]propane, palladium acetate, Sulfuric acid, *p*-benzoquinone, deuterated-hexafluoroisopropanol (*d*-HFIP), calcium chloride (CaCl₂), zinc chloride (ZnCl₂), and lithium chloride (LiCl) were purchased from Sigma-Aldrich Co. and ethylene and carbon monoxide gas were supplied by Energen Co. and Air Liquid Co., respectively. All reagents and solvents were used as received without any further purification.

Preparation of poly(1-oxotrimethylene) (POTE)

1,3-Bis[di(2-methoxyphenyl)phosphino]propane (0.0359 g, 0.067 mmol) in 12.5 mL of acetone was mixed with palladium acetate (0.0126 g, 0.056 mmol) in 12.5 mL of acetone before stirred for 1 h. Then sulfuric acid (0.368 g, 3.752 mmol) and *p*-benzoquinone (3.04 g, 28.125 mmol) were added to the reaction mixture to form a homogeneous solution. 25 mL of this solution, 2.2 L of methanol and 0.3 L of water were added into a 5 L autoclave, and then ethylene and carbon monoxide were injected into the autoclave at a 1:1 molar ratio. The amount of each component and the solvent added were determined in the previous works[11-12]. The reaction mixture was heated at 80 °C for 3 h and the product was washed several times with methanol followed by subsequent drying at 80 °C for 16 h. ¹H NMR (CDCl₃/*d*-HFIP = 50/50 weight ratio, δ in ppm): 2.75 (s, 4H). The intrinsic

viscosity ($[\eta]$) measured in HFIP was 5.7 dL/g at 25 °C.

Preparation of Fibers

8.5 wt % of polymer solution was prepared by dissolving 10.32 kg of polymer in an aqueous solution containing a mixture of metal salts (CaCl₂/ZnCl₂/LiCl/H₂O = 33.30/24.42/11.00/42.18 kg (30/22/10/38 wt. ratio)) at 50 °C. When the ZnCl₂ and CaCl₂ were used for the salt mixture to prepare the polymer solution, phase-separation was observed and fine fibers were obtained as reported by others[11]. With the introduction of 10 wt % LiCl, similar phase-separation phenomenon was also observed and moreover higher solubility with low viscosity solution could be obtained. Thus the polymer solution could be more easily transported through heated pipes at 80 °C in the wet spinning process. After filtration, the solution flows into a spinneret containing 504 capillaries with a diameter of 0.15 mm and an aspect ratio (capillary length/diameter) of 1. The solution spurt out from the end of the capillary to forms a fiber at an extrusion speed of 8 ~ 9 m/min. The extruded fibers were then soaked into a cold aqueous solution (coagulation bath) containing 10 wt % of salts (CaCl₂/ZnCl₂/LiCl = 30/22/10 wt. ratio) to obtain an undrawn fiber. The coagulated fiber was taken up by 11.2 m/min Nelson roll then passed through a 0.5 wt% hydrochloric acid bath, washed by a pressurized water gun, and the undrawn fiber was dried using a hot steam at 220 °C for 12 h. After drying, the undrawn fiber was processed by the draw winding system. Such a system was used for a continuous drawing of fibers by roller rotating with different velocities, and the draw

ratio was hence defined at a predetermined temperature maintained by hot air circulation. The machine consists of two drawing zones with three sets of rolls and the lengths of the drawing zone are 8 and 12 m, respectively. In the drawing zone, undrawn fiber was isolated from any other material except the roller. The first set of rolls was rotated at a linear speed, and the third set was maintained at a speed that would give the desirable total draw ratio. The second roll set was kept at a speed between the other two, usually closer to that of the third set than the first, so that the major draw took place in the first drawing zone. The drawing condition of poly(1-oxotrimethylene) (POTE-X, where X is the draw ratio) is listed in Table 1. The maximum draw ratio was kept at 16 because the fibers broke off at any draw ratio larger than 16.

Measurements.

The molecular weight and polydispersity index were measured by a Waters 515 GPC equipped with a Waters2414 RI detector. HFIP was used as a solvent and monodisperse poly(methyl methacrylates)s were used as the standards. Differential scanning calorimetry (DSC, Universal V4.1D TA Instruments) was carried out in a nitrogen atmosphere at the heating and cooling rates of $5\text{ }^{\circ}\text{C min}^{-1}$. The transition temperatures and enthalpy changes were obtained from the second heating scan. X-ray diffraction experiments were performed at the 3C2 beam line at the Pohang Accelerator Laboratory (PAL).

The mechanical properties were measured using a universal testing machine (UTM,

Instron 5565 Standard). The testing fiber specimens were prepared according to the ASTM standard. The mechanical properties of the fiber samples were measured in air at 23 °C under a 45 % relative humidity with a gauge length head speed of 100 mm/min. The tensile strength, modulus, elongation at break, and maximum load values were also investigated and measured more than 5 times and the data listed in the manuscript are the average values from each sample.

3.3. Results and Discussion

Poly(1-oxotrimethylene) having high molecular weight about 1,000,000 was prepared by gas polymerization using a palladium catalyst system, containing a mixture of palladium acetate, 1,3-bis[di(2-methoxyphenyl)phosphino]propane, sulfuric acid, and *p*-benzoquinone. The formation of poly(1-oxotrimethylene), an alternating copolymer from ethylene and carbon monoxide, using the palladium catalyst system was confirmed by a ¹H NMR spectrum using CDCl₃/*d*-HFIP (50/50 weight ratio) as a solvent; only a singlet peak at 2.75 ppm for the protons from the four backbone carbons was observed. After the wet spinning process, undrawn fiber was dried under various temperatures and the changes in tensile strength were observed at different draw ratios in order to optimize the fiber production condition (Figure 1). The tensile strength of the fiber increases as the drying temperature increases from 150 to 220 °C, while it decreases when the drying temperature is 250 °C. Kato *et al.* have reported the relationship between the tensile strength and draw ratio, when undrawn fibers are prepared at different drying temperatures, coagulation bath temperatures, metal solution compositions, and/or dissolution times[11-13]. They reported that the maximum strength increased with the increase of the drying temperature to 250 °C, and then both the maximum draw ratio and maximum strength decreased with any further increase of temperature. We also found that the maximum tensile strength increased with the increasing drying temperature. However when we used 250 °C as the drying temperature, POTE fiber was damaged during the

drying and drawing steps. When the fiber preparation condition was unsuitable, the fibers were broken during the drawing step. In case of the 250 °C drying condition, POTE fiber was damaged during the drying step and drawing step, then the high draw ratio was not available. This discrepancy might be caused by the different heating system. Hot air drying system (non-contact drying) used in our drying step appears to have higher heat transfer efficiency than that of hot plate system used by Kato *et. al.* Other factors such as composition of aqueous solvent and/or melting temperature of undrawn fiber might also lead to the discrepancy, despite the difference in heating systems is probably the major factor. We also observed the deformation of the fiber structure at 250 °C using X-ray diffraction which is shown in the later part of this manuscript.

Figure 2 shows cross-sectional SEM photographs of undrawn fibers before and after drying at 220 °C. The fiber before drying consists of many voids which can act as defects during the drawing step. These defects may result in lower mechanical properties of the drawn fibers. After the heat treatment at 220 °C, voids were removed and thus dense and homogeneous fibers could be formed. Based on the above results, 220 °C was chosen as the desirable temperature used for drying and drawing steps to obtain the POTE-Xs.

Figure 3 illustrated the DSC traces of the POTE-Xs obtained from the second heating scan at a heating rate of 5 °C min⁻¹ and large endothermic peaks were observed in the range of 250 to 265 °C. Table 1 lists the melting temperature (T_m), heat of fusion, and crystallinity of the fibers that calculated from the heat of fusion by referring the heat of fusion of 239 J/g as 100% crystalline. The wet spinning process was found to decrease T_m ,

while the drawing process increased T_m . For example, the T_m values of POTE-0 and POTE-7 are 254.3 and 255.6 °C, respectively which are smaller than that of POTE powder (264.1 °C). However T_m values of POTE-10 to -16 is larger than that of the powder sample. The melting temperature of polymeric material is affected by many factors such the molecular weight, crystallinity, ordering of the structures, impurity, and others. Also the solvent such as water and methanol used for the polymerization and purification of the polymers could affect the melting temperature because polymers can be ordered during the solvent evaporation steps. Therefore possibly POTE powder having largest molecular weight and some degree of ordering generated during solvent evaporation steps have higher melting temperature than POTE-0 and POTE-7 having smaller molecular weight, while POTE-10 to POTE-16 shows larger melting temperature than the powder possibly because of their larger degree of crystallinity as shown in Table 1[3,12]. The heat of fusions increases with the increasing draw ratio since the drawing step can increase the order of crystal structure by molecular rearrangement resulting from the wet spinning step[3,12]. As a result the heat of fusion and crystallinity of POTE-16 is much higher than others. The weight average molecular weight (M_w) and polydispersity index (PDI) of POTE-Xs determined by GPC are also listed in Table 1. The M_w and PDI decrease with increasing draw ratio due to the cleavage of the backbone structure as reported by others[12].

The poly(1-oxotrimethylene) has been known to have two distinct crystalline structures that are α and β -phases; the α -phase crystal is denser than the β -phase crystal, and their

packing energy values of the α - and β -phases were reported to be -697 and -656 J/g, respectively [3,12,17]. The crystalline structures of our samples were studied by X-ray diffraction experiments and the results are shown in Figures 4 and 5. Figure 4a shows the influences of draw ratio on the crystalline structures at room temperature. Figures 4b and 4c show the effect of temperatures on the crystalline structures with fixed draw ratio, 7 and 16, respectively. The diffraction peaks in Figure 4 were assigned referring to the results obtained by others[2-5]. A distinctive diffraction peak centered at 21.4° has been known to be from 110 planes of both α - and β -phases, while 25.3° and 30.9° peaks are from 200 and 210 planes of the α -phase, respectively, and the 28.5° and 37.0° peaks are from 210 and 212 planes of the β -phase, respectively. Therefore the drawn fibers (POTE-7, 10, 14, 16) mostly have the more dense α -phase, while the powder sample (POTE) and undrawn fiber (POTE-0) have the unoriented β -phases at room temperature. Therefore the less dense β -phase existing in the undrawn fiber is mostly converted to the dense α -phase by the drawing process. Two dimensional X-ray photographs shown in Figure 5 indicates that POTE and POTE-0 containing β -phases have poorly oriented crystal structures showing circle patterns, while the drawn fibers containing mostly α -phase have highly oriented crystal structures giving rise to sharp peak spots. As shown in Figure 4b for POTE-7 and Figure 4c for POTE-16, when the drawn fibers are heated, α -phase disappears while β -phase appears at around 100-120 °C. Therefore the small endothermic peaks observed at 117.2, 110.8, 109.3, and 105.9 °C from the DSC curves of POTE-7, 10, 14, and 16, respectively, could be assigned as the phase transition temperatures from α -

phase to β -phase for each sample.

GPC results in Table 1 clearly indicate that the increase of the draw ratio decreases the molecular weight. Therefore the drawing process cleaves the polymer backbone structures, while it increases the heat of fusion, crystallinity, and ordering of the fiber structure. For example, the crystallite size and crystalline orientation were also found to increase with increasing draw ratio as shown in Table 2. The crystallite size of drawn fibers was calculated from the full width at half maximum (FWHM) of the peak at 21.4° and the crystalline orientation was calculated using eq. (1) where H is a FWHM from a circumferential intensity plot of 21.4° .

$$\text{Crystalline orientation (\%)} = \{(180 - H) / 180\} * 100 \quad (1)$$

Figure 6 shows the changes of crystallinity and crystalline orientation with respect to the draw ratio. The drawn fiber has much higher crystallinity and larger crystalline orientation values than the undrawn fiber, POTE-0. The crystalline orientation value increases slightly when the draw ratio increases from 7 to 14 and those of POTE-14 and POTE-16 are almost identical within experimental error. In contrast, the crystallinity of the drawn fibers increases significantly with the increase of the draw ratio from 14 to 16. Similarly the increase of crystallinity and crystalline orientation with the increase of the draw ratio is commonly observed in the polymer fiber systems[18,19], while the reason for the large increase in the crystallinity with the same crystalline orientation value from

14 to 16 is still unclear. However, it is very clear that the drawn fibers prepared from the draw ratio of 14 to 16, POTE-14 to POTE-16, have different mechanical properties as shown in the next paragraph of this manuscript. The structural and mechanical parameters of polymers discussed here, such as molecular weight, polydispersity index, melting temperature, heat of fusion, crystal phase, crystallinity, crystallite size, crystalline orientation, and mechanical property are all closely related to each other although discrepancies are observed in the case of POTE-14 and POTE-16[20-25].

We could prepare POTE fibers having denser packing structure without any voids, if any, as shown in Figure 2 from the optimum drying temperature at 220 °C. The following drawing steps could produce the fibers having α -phase, and it increased the crystallinity and crystalline orientation although the molecular weight decreased. Based on the above considerations, mechanical properties of a series of POTE fibers were compared with other commercial fibers for tire cord application.

Table 3 shows the mechanical properties of our samples as a function of draw ratio including commercial fibers such as poly(ethylene terephthalate) (PET, HSP-40), Nylon6, Rayon (S-3), and Aramid. For the POTE series, the increase of the draw ratio enhances the tensile strength and modulus, while reduces the elongation at break and maximum load as expected[26,27]. Therefore, the changes in tensile strength and modulus generally are influenced by the changes in melting temperature, crystallinity, crystallite size, and crystalline orientation to a certain extent, although a clear explanation of their relationship is still not possible. The decrease of the elongation at break and maximum load with the

increase of the draw ratio is directly related with the decrease of the molecular weight because polymers with smaller molecular weight normally have less entangled structures and thus decreased elongation at break and maximum load[26]. The maximum tensile strength and modulus were observed for POTE-16, which is prepared with a maximum draw ratio. These values are larger than those of PET, Nylon 6, and Rayon fibers, but smaller than that of Aramid fiber. On the contrary, the elongation at break of POTE-16 is smaller than those of PET, Nylon 6, and Rayon fibers, but larger than that of Aramid fiber. The load at maximum of POTE-16 is smaller than all of the commercial fibers studied here. Currently we are trying to apply the drawn POTE fiber as tire cord, where PET and Nylon 6 fibers shown in Table 3 are most commonly used for this purpose. Since the tensile strength and modulus of the highly drawn POTE fibers are larger than those of PET and Nylon 6 whereas elongation at break of POTE is smaller, POTE fibers can be potentially utilized as tire cord materials with superior properties. Such work is under progress and the result will be reported shortly.

3.4. Conclusions

High molecular weight poly(1-oxytrimethylene) (POTE) was successfully synthesized using a palladium catalyst system and its fibers having different draw ratios were prepared for the systematic study of crystalline structure and mechanical properties. The increase of the draw ratio improves the crystallinity, melting temperature, tensile strength, and modulus, while it decreases the molecular weight and elongation at break. Since the tensile strength and modulus of the drawn POTE fibers are larger than those of other commercial fibers for tire cords such as PET and Nylon 6, POTE fibers can be a very promising alternative for tire cords.

Table 3-1. Drawing conditions, molecular weight, polydispersity index and thermal properties of POTE-Xs

Sample	Draw ratio	M _w	PDI	Draw temperature (°C)	T _m (°C)	Heat of fusion (J/g)	Crystallinity (%)
Powder	-	1,087,000	3.13	-	264.1	115.4	48.3
POTE							
POTE-0	-	1,014,000	2.90	-	254.3	112.3	47.0
POTE-7	7	588,000	2.65	235	255.6	134.6	56.3
POTE-10	10	434,000	2.58	250	264.4	136.0	56.9
POTE-14	14	385,000	2.52	260	264.8	137.4	57.5
POTE-16	16	330,000	2.46	265	265.0	149.4	62.5

Table 3-2. X-ray results of POTE-Xs

Sample	FWHM ^a	Crystallite size (nm)	FWHM ^b	Crystalline orientation (%)
POTE-0	1.17	8.05	47.18	73.8
POTE-7	1.04	9.05	9.89	94.6
POTE-10	0.92	10.28	7.33	95.9
POTE-14	0.90	10.51	5.53	96.9
POTE-16	0.89	10.67	5.74	96.9

^a FWHM from the peak centered at 21.4°

^b FWHM from a circumferential intensity plot of 21.4°

Table 3-3. Mechanical properties of POTE-Xs and commercial fibers

Sample	Tensile strength (g/denier)	Modulus (g/denier)	Elongation at break (%)	Load at maximum (kg)
POTE-7	8.5	123.7	8.2	11.8
POTE-10	10.6	234.6	5.8	10.3
POTE-14	11.0	302.1	4.3	8.0
POTE-16	13.4	369.8	4.2	7.6
PET ^a	8.8	110.0	12.0	13.4
Nylon6 ^b	9.5	55.0	20.0	12.0
Rayon (S-3) ^c	6.8	155.0	10.5	10.8
Aramid ^d	22.0	500.0	3.5	33.0

^a PET tire cord HSP-40 (Non-AA) supplied by Hyosung Co.

^b Nylon6 tire cord supplied by Hyosung Co.

^c Rayon super-3 supplied by Cordenka Co.

^d Aramid ALKEX type : AF1000 supplied by Hyosung Co.

Figure 3-1. Changes in tensile strength with respect to draw ratio at different drying temperatures

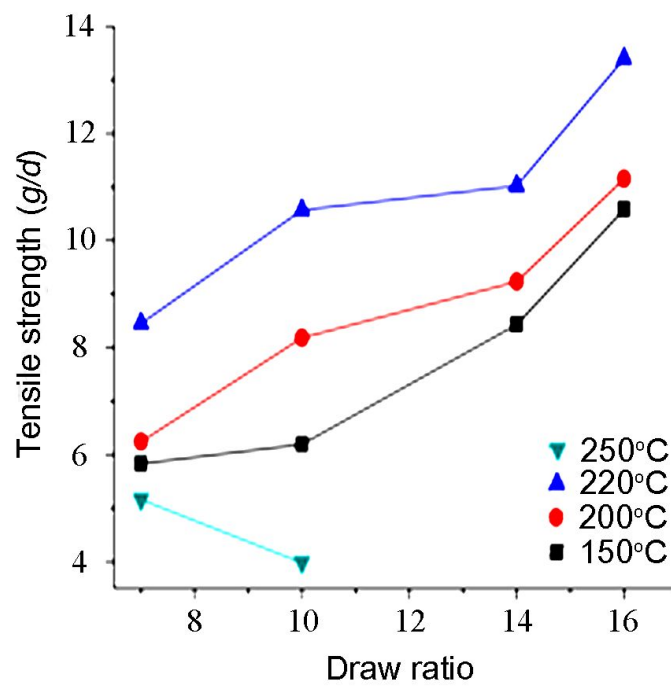


Figure 3-2. Cross-sectional SEM photographs of POTE fibers (a) before and (b) after drying at 220 °C

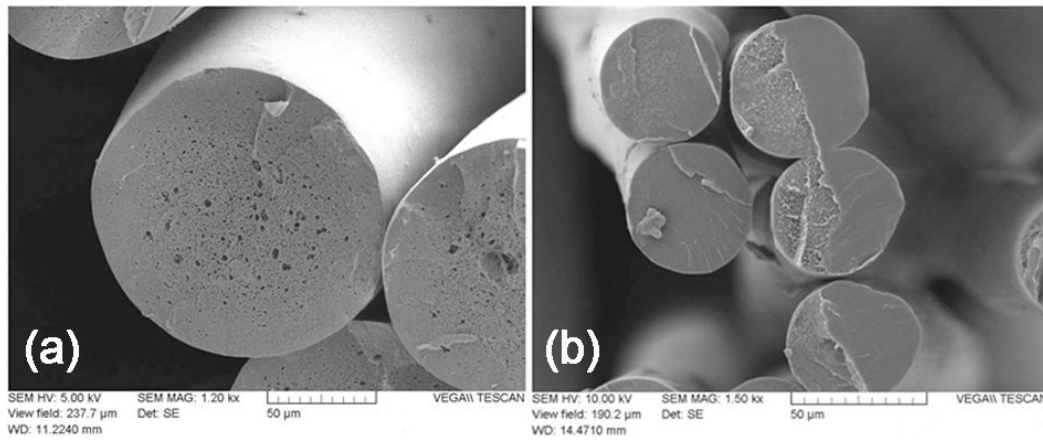


Figure 3-3. DSC thermograms of POTE-Xs

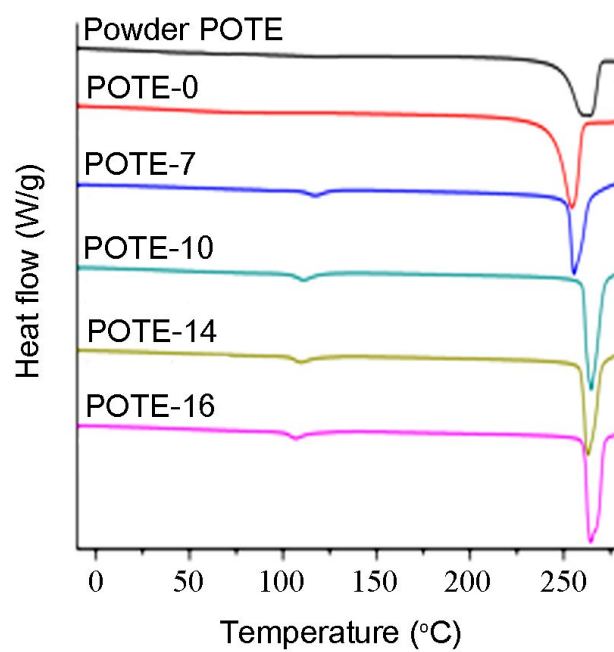
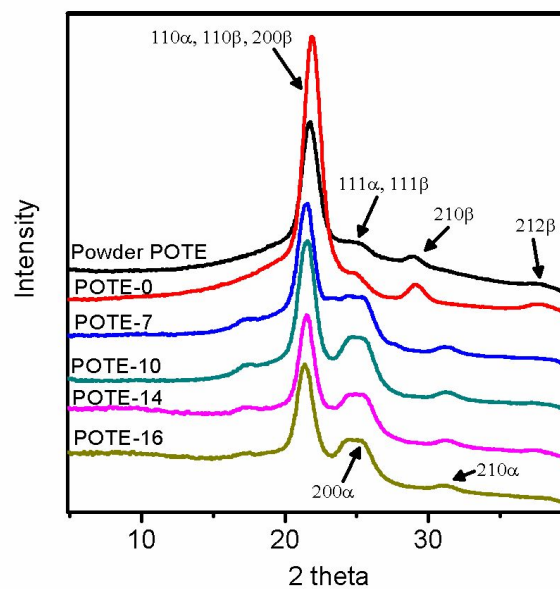
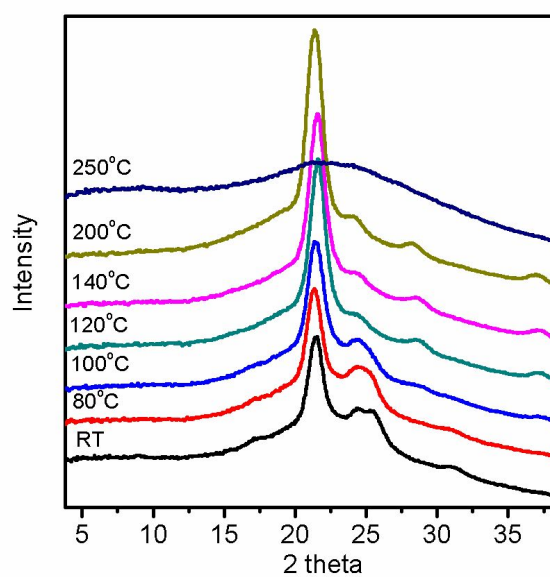


Figure 3-4. X-ray diffraction patterns of (a) POTE-Xs at room temperature and those of (b) POTE-7 and (c) POTE-16 at different temperatures.

(a)



(b)



(c)

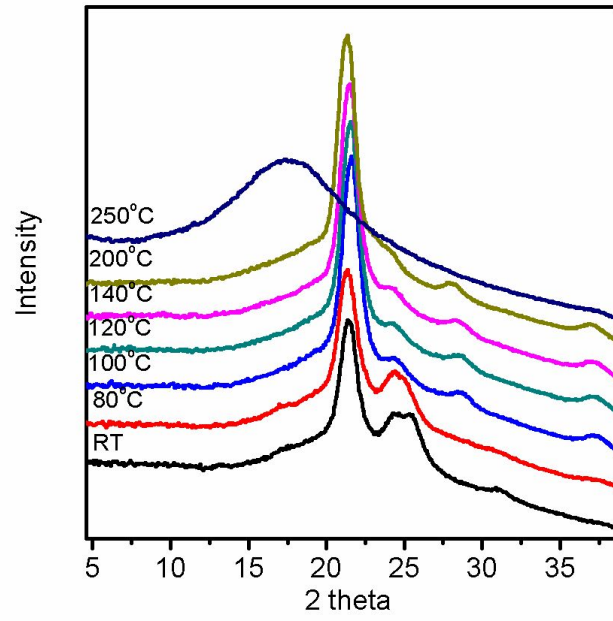


Figure 3-5. Two-dimensional X-ray diffraction photograph of POTE-Xs: (a) powder POTE, (b) POTE-0, (c) POTE-7, (d) POTE-10, (e) POTE-14, (f) POTE-16 at room temperature.

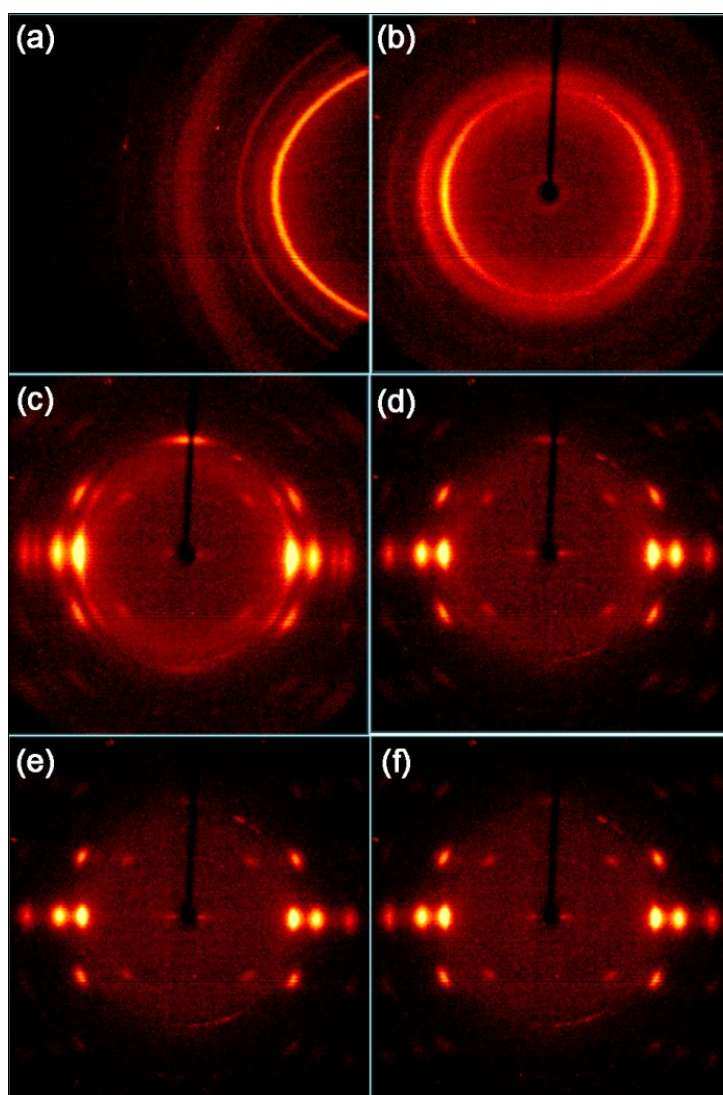
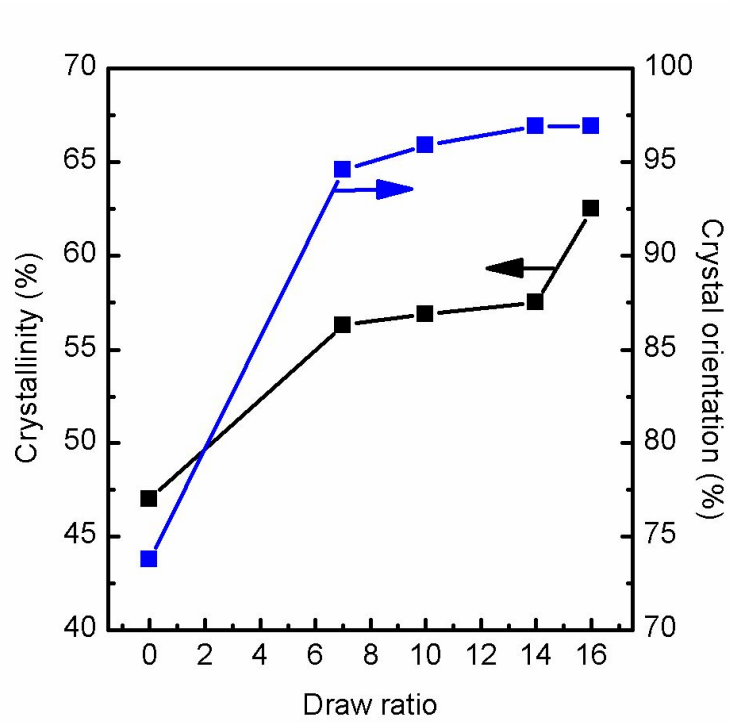


Figure 3-6. Changes in crystallinity and crystalline orientation with respect to draw ratio



3.5. References

- [1] E. Drent, and P. H. M. Budzelaar, Chem. Rev., **96**(1996) 663.
- [2] B. J. Lommerts, E. A. Klop, and J. Aerts, J. Polym. Sci. B Polym. Phys.,
31(1993)1319.
- [3] E. A. Klop, B. J. Lommerts, J. Veurink, J. Aerts, and R. R. Van Puijenbroek, J. Polym.
Sci. B Polym. Phys., **33**(1995)315.
- [4] A. J. Waddon, N. R. Karttunen, and A. J. Lesser, Macromolecules, **32**(1999) 423.
- [5] J. M. Largaron, M. E. Vickers, A. K. Powell, and N. S. Davidson, Polymer,
41(2000)3011.
- [6] E. Drent, and W. W. Jager, Polym. Mater. Sci. Eng., **74**(1997)100.
- [7] C. E. Ash, and J. E. Flood, Polym. Mater. Sci. Eng., **74**(1997)110.
- [8] J. G. Bonner, and A. K. Powell, Polym. Mater. Sci. Eng., **74**(1997)108.
- [9] M. M. Brubaker, D. D. Coffman, and H. H. Hoehn, J. Am. Chem. Soc.,
74(1952)1509.
- [10] Y. Chatani, T. Takizawa, S. Murahashi, Y. Sakata, and Y. Nishimura, J. Polym. Sci.,
55(1961)811.
- [11] T. Morita, R. Taniguchi, T. Matsuo, and J. Kato, J. Appl. Polym. Sci., **92**(2004)1183.
- [12] T. Morita, R. Taniguchi, and J. Kato, J. Appl. Polym. Sci., **94**(2004) 446.
- [13] T. Morita, M. Adachi, and J. Kato, J. Appl. Polym. Sci., **96**(2005)1250.
- [14] T. Morita, and J. Kato, J. Appl. Polym. Sci., **100** (2006)3358.
- [15] Y. Zuigyo, Tire Sci. and Technol., **35**(2007)317.

- [16] P. Gupta, J. T. Schulte, J. E. Flood, J. E. Spruiell, *J. Appl. Polym. Sci.*, **82**(2001)1794.
- [17] J. G. Bonner, A. K. Powell, *Polym. Mater. Sci. Eng.*, **74**(1997)108.
- [18] Y. Liu, J. Li, Z. J. Pan, *Adv. Mater. Res.*, **175**(2011)90
- [19] A. Lund, B. Hagstrom, *J. Appl. Polym. Sci.*, **116**(2010)2685.
- [20] B. Wu, Y. Gong, G. Yang, *J. Mater. Sci.*, **46**(2011)5184.
- [21] N. Han, X.-X. Zhang, W. Y. Yu, X.-Y. Gao, *Macromol. Res.*, **18**(2010)1060.
- [22] C. H. Lee, Y. J. Cha, S. Choe, *J. Ind. Eng. Chem.*, **4**(1998)161.
- [23] Y. A. Kang, K. H. Kim, H. H. Cho, T. Kikutani, *J. Appl. Polym. Sci.*, **95** (2005)212.
- [24] T. P. Mohan, J. Kuriakose, K. Kanny, *J. Ind. Eng. Chem.*, **17**(2011)264.
- [25] W.-S. Kim, D.-H. Lee, I.-J. Kim, M.-J. Son, W. Kim, S.-G. Cho, *Macromol. Res.*, **17**(2009)776.
- [26] S.-K. Kim, T.-H. Kim, J.-W. Jung, J.-C. Lee, *Polymer*, **50**(2009)3495.
- [27] Y. Yoo, M. W. Spencer, D. R. Paul, *Polymer*, **52**(2011)180.

Chapter 4

A Study on the Preparation and Characteristics of Glass Fiber-Reinforced Polyolefin Ketone Composites

4.1. Introduction

Polyolefin ketone polymer, synthesized from carbon monoxide and olefin used as monomer, provides excellent mechanical strength, chemical resistance, abrasion resistance, gas barrier property, high fracture toughness and impact resistance, and therefore has been intensively researched due to its extensive range of applications such as fiber, engineering plastic and composites. Specifically, there is a surging demand for polyolefin ketone polymer, which outperforms the existing materials in terms of mechanical strength, rubber adhesion, and price competitiveness, etc., in the fields of rubber-reinforced fibrous composite materials, or tire code, mechanical, electric, electronic parts[1-2]. Polyolefin ketone polymer exhibits a variety of physical properties and finds extensive applications in a wide range of fields, depending on the type of olefin used as monomer. In particular, linear alternating copolymer composed of carbon monoxide and ethylene are most commonly used along with terpolymer composed of carbon monoxide, ethylene, and propylene. Researches have been variously conducted to develop the engineering process incorporating the methodologies that involve the physical properties and structure of these polymers [3-5].

Polymer composites can be produced by introducing the reinforcement into the polymer through simple engineering process and has excellent mechanical properties comparable to those of inorganic matters such as metal and ceramic.

Moreover, polymer composites have additional properties, such as corrosion resistance, high elasticity, etc., and therefore have found extensive applications in various fields. Among the most typical fiber-reinforced materials (fibrous reinforcement) which are introduced into those composite materials mentioned above include glass fiber, carbon fiber, aramid fiber, and others.

Specifically, glass fiber has the advantage of low cost and easiness of processability, as well as fulfill major requirements, and resultantly has been constantly used as the optimized reinforcement in universal composite materials [6-10]. Generally, the fibrous reinforcement effect of fiber-reinforced composites is mostly determined by the strength, size, dispersion of the reinforcement per se, and the interfacial properties between the applied reinforcement and polymer matrix is considered the most important factor. Although the polymer or reinforcement has the bonding force beyond a certain degree, their interfacial surface determines the overall uniformity of composite material which immediately affects the physical properties of composites. Thus, various surface treatment methods have been proposed to achieve the enhancement of interfacial adhesion, and the glass fiber with proper surface treatment in various polymer matrixes has been made commercially available.

In this study, the surface-treated glass fiber was introduced to develop the composite material providing the enhanced physical properties of polyolefin ketone polymer that can find application as the engineering plastic. Polyolefin ketone was

synthesized from carbon dioxide, ethylene, and a small amount of propylene, and the glass fiber – treated by urethane and amino silane or urethane, epoxy, and amino silane – was used as reinforcement. Interfacial structure analysis was carried out, using the scanning electron microscopy (SEM), to determine the compatibility of polymer matrix and glass fiber. This study was intended to examine the applicability of polyolefin ketone polymer as the engineering plastic by identifying the mechanical properties of composites based on each glass fiber.

4.2. Experimental

Reagent

All reagents used in the experiment were purchased from Aldrich, such as 1,3-Bis[di(2-methoxyphenyl)phosphino]propane(BDOMPP), palladium acetate($\text{Pd}(\text{OAc})_2$), Trifluoroacetic acid(TFA), hexafluoroisopropanol, etc. The carbon monoxide gas and ethylene, the monomer used in the polymerization, were purchased from Energen and Air Liquide, and the propylene was purchased from the Ulsan plant of Hyosung (PP-DH PU).

Besides, XL-1 (Chemtura), Calcium hydroxyapatite (Budenheim), Nucrel N1183C, the copolymer of methacrylic acid and ethane, etc., were purchased to prepare the specimen.

The glass fiber used as the reinforcement of polyolefin ketone polymer, the chopped strand glass fiber- which underwent the surface treatment with urethane and amino silane or urethane, epoxy, and amino silane – was purchased from Owens Corning Korea.

The nomenclature of the purchased fiber glass was based on the product name of glass fiber, fiber diameter and length. For example, 910-13P-4 means the glass fiber of 910 type that uses the urethane and amino silane as binder with the fiber measuring 13 μm in the diameter and 4mm in length. All reagents and solvents were used exactly in the condition that they were purchased without any refining process.

Synthesis of polyolefin ketone polymer

The terpolymer composed of carbon monoxide, ethylene, and propylene was

polymerized in the presence of catalyst compound combined with Pd(OAc)₂, BDOMPP, and TFA at the ratio of 1:1.2:20. [11-13] In the first place, BDOMPP, the ligand, was melted in the acetone at the room temperature and intermixed with Pd(OAc)₂ to ensure perfect melting. Then, the catalyst was produced by adding the TFA 5 minutes prior to the use of the polymerization container for the purpose of inducing the activity of catalyst. The seed powder, methanol, and water were injected into the reaction container beforehand to achieve the gas phase polymerization, and the reaction container temperature was adjusted after feeding the necessary amount of propylene (liquid) into the container. The propylene concentration of copolymer used in this experiment was set to 6 % of the total polymer concentration, and the optimal polymerization temperature was derived by adjusting the polymerization temperature to 84 – 94 °C. After the propylene was fed into the container, the pressure of the polymerization container was maintained at 56 bar while feeding the carbon monoxide and ethylene gas into the container at the ratio of 1:1. Upon completion of the gas feeding and the adjustment of temperature and pressure, the pre-manufactured catalyst was put into the catalyst reaction container. The reaction continued for 6 hours. To terminate the reaction, the gas was discharged immediately upon lowering the temperature of the reaction container. After the termination of reaction, the solvent and polymer were separated and collected from the polymerized matter using the centrifugal separation. Then, solvent and polymer were dried for 14 hours at 80 °C in the nitrogen atmosphere. The propylene concentration of copolymer and synthesis of polymer was determined by using ¹H NMR spectrum.

^1H NMR ($\text{CDCl}_3/d\text{-HFIP} = 50/50$ weight ratio, δ in ppm): 1.17 (m, 3H), 1.95 (m, 6H), 2.75 (m, 4H), 3.72 (s, 3H).

Preparation of polyolefin ketone polymer & composites specimen

To ensure effective formation of specimen, XL-1, calcium hydroxyapatite, and Nucrel N1183C were added by 0.2, 0.3, and 0.2 wt%, respectively, in the synthesized polyolefin ketone polymer. The specimen was produced by varying the composition of the surface-treated 'glass fiber' at the ratio of 15 or 30 wt%.

ISO 3167 multi-purpose specimen (Center Section: 80 x 10 x 4 mm: tension specimen, 64 x 10 x 4 mm: flexural specimen, $r = 0.25$ mm, 80 x 10 x 4mm: Charpy impactspecimen) was produced by using the hydraulic injection molding machines NT-III (mould claming force 80 Ton) of WOOJIN SELEX.

The temperature was set to 240 °C and the injection speed was set to 60 mm/s. The holding pressure was set to 70 bars, while the hold-pressure time was set to 15 seconds for injection.

The obtained specimen was analyzed after being left unattended for 24 hours in the constant temperature/humidity room at the temperature of 23 °C and the relative humidity of 50%.

Device

In relation to the ^1H NMR, DSC, and SEM images, the data were obtained by using 300 MHz JEOL JNM-LA 300, Universal V4.1D TA Instruments, and JSM-6700F of JEOL. The intrinsic viscosity was measured at 25 °C using the Ostwald Viscometer by dissolving the polymer in the hexafluoroisopropanol.

The mechanical properties of polyolefin ketone polymer and the glass fiber-reinforced composites were measured by using the instron. The tensile strength and tensile modulus were measured at a speed of 50 mm/min as per ISO 527, while the flexural strength and flexural modulus were measured at a speed of 2 mm/min as per ISO 178. The charpy impact strength was measured in accordance with the procedures set forth by ISO 179-1. All numbers presented herein were obtained by averaging the results of the measurements performed more than 5 times.

4.3. Results and Discussion

Synthesis of polyolefin ketone polymer

Polyolefin ketone polymer, which has strong mechanical properties in wide temperature range, is designed and synthesized in such a way as to be suited for various fields of applications[1-5]. This research group synthesized the linear alternating polyolefin ketone copolymer which had been formed by carbon monoxide and ethylene in the preceding studies, analyzed its structure through the elongation, and confirmed its applicability in the tire code sector[13].

In this study, the polyolefin ketone polymer for the engineering plastic application was synthesized by additionally introducing the propylene into the polymer which had been synthesized beforehand.

This terpolymer exhibits a decrease in the melting temperature of polymer to a range between 210 and 250 °C with the increasing propylene concentrations, and has excellent physical properties, impact strength/resistance, chemical stability and processability, and therefore has been vigorously researched[3-4]. In this study, the propylene concentration was set to 6 mol%, and various glass fibers were added into the synthesized polymer to determine the mechanical properties and applicability as the composite material for the engineering plastic.

The synthesis of polyolefin ketone polymer was already introduced by many different research groups, and is also presented in the patent[1-5, 11-13]. In this study, the

manufacturing method, already known, was employed in such an optimized way as to enable the synthesis of large amounts of polymer and it was confirmed that the polymerization temperature, catalyst, composition, and reaction pressure – which were presented in the experiment – corresponded to the optimal values. Figure. 1 shows the structure of the synthesized polyolefin ketone polymer and the materials used for the synthesis, while Fig. 2 shows the NMR spectrum. The propylene concentration in polymer was calculated based on the peak located near 1.15 ppm from propylene and the peak integrals near 2.75 ppm which can be simultaneously checked from the propylene and ethylene.

Polyolefin ketone terpolymer exhibited a difference in polymer viscosity and yield, depending on the polymerization temperature, when other conditions of polymerization were constant. Fig. 3 presents the graphic representation of intrinsic viscosity of polymer and activity of palladium used as catalyst based on the polymerization temperature. The activity of palladium was calculated by dividing the quantity of the obtained polyolefin ketone polymer per gram of palladium catalyst by the time unit. As shown in the Fig.3, the reactivity of catalyst sharply increases with the rising temperature of polymerization and declines after peaking at 92 °C. Such decrease in the activity of catalyst and the consequent decline in the yield of polymer are considered attributable to the excessive energy applied at a temperature beyond a certain level, which in turn prompts the termination reaction of methanol – used as solvent – and palladium catalyst, although the activity of catalyst increases as the temperature rises. In other words, the increasing

temperature leads to an improvements of activity and side reaction of catalyst, and the yield of synthesized polymer – which are determined by those two elements – reach the peak at 92 °C. In the experiment, it was observed that the intrinsic viscosity decreased linearly as the polymerization temperature increased, and the primary trend line which shows the degree of decrease can be derived using the following formula:

$$\text{Intrinsic Viscosity (dL/g)} = -0.11 \times \text{polymerization temperature} + 11.19 \quad (1)$$

As mentioned above, the increase in the polymerization temperature leads to an increase in the activity of catalyst which in turn results in the increased yield rate. However, molecular weight decreases due to the increase in the termination reaction with the solvent, besides the polymerization monomer, and resultantly, the intrinsic viscosity declines.

The specimen was produced by adding the antioxidants, the melting stabilization agent, XL-1, calcium hydroxyapatite, and Nucrel N1183C – which work as lubricating oil – into the polymer which had been synthesized according to the procedure described above, using the 2-axis screw, and was used for experiment later.

Introduction of glass fiber

The glass fiber used in this study was the chopped strand glass fiber of which surface was treated with the binder, and related details are presented in the Table 1. The

nomenclature of the glass fiber was based on the product name, fiber diameter and length. All were OCF class products manufactured by Owens Corning and used exactly in the condition that they were purchased without any treatment. In addition, various types of glass fiber were used to determine their properties based on the diameter and length of fiber and binder. The glass fiber was produced by passing it through the roll plastered with binder, and cut into regular-sized pieces through the roll fitted with a cutter. For the experiment, this study selected and used the glass fiber containing the amino silane, urethane, and epoxy – known to have excellent compatibility with polyolefin ketone – as binders based on the results of existing studies[11-12]. The glass fiber of 910 type used the amino silane, urethane as the binders, while the glass fiber of 923 and 995 types used the amino silane and urethane and epoxy as binders. Specific information related to the contents by composition is undisclosed. The specimen was formed with a mixture of 15 or 30 wt% based on the polymer which was synthesized beforehand.

The compatibility between the polymer and glass fiber is the most important factor in successfully producing the composites. The compatibility is determined by the binder applied mainly to the surface of glass fiber beforehand, and the type and the applications of the reinforced polymer are determined by the type of binder which is also known as the sizing material or coupling agent.

The compatibility with binder shows the degree of adhesion between polymer and glass fiber. Higher degree of adhesion makes the excellent mechanical properties of glass fiber transmitted to the polymer well. This study used the glass fiber containing the amino

silane and urethane – which is known to have excellent compatibility with the polyolefin ketone polymer – as binders. To determine the difference in binders, a comparative experiment was conducted using the glass fiber that additionally had the epoxy and the same diameter and length.

Depending on the type of glass fiber mixed in the polyolefin ketone polymer, the composites were named differently; 910-13P-4 was named as Composite 1, 910-10P-4 as Composite 2, 910-10P-3 as Composite 3, 923-10C-4 as Composite 4, and 995-10P-4 as Composite 5.

In the comparative experiment, the length and diameter of the glass fiber were also considered as the elements that would significantly affect the physical properties of composites. The glass fiber with proper size is required, considering that the desired strength cannot be obtained if the diameter of the fiber is too small and the fiber with excessively large diameter would have an increasing mass to achieve the required strength. The glass fiber diameter suitable for the composites is known to range somewhere between $5\mu\text{m}$ and $20\mu\text{m}$, and particularly, the preferred diameter is in the range between $8\mu\text{m}$ and $15\mu\text{m}$ [11]. Materials with excellent mechanical properties can be sometimes obtained in some applications if the fiber has a large and regular length. However, the chopped strand glass fiber is preferred in the glass fiber-reinforced composite applications, and the commonly-used fiber measures 2.5 to 2.5mm. Long fibers and short fibers have their own advantages. However, excessively long fiber causes

degradation of processability in the mixture with polymer, and excessively sort fiber prevents the achievement of the desired physical properties[11].

Identification of the interfacial properties of glass fiber and polymer

As mentioned before, the compatibility between glass fiber and polymer, which varies depending on the type of binder, is very important factor in determining the physical properties of composites. The compatibility was characterized by observing the fracture surface of composites with the scanning electron microscopy (SEM). The Fig. 4 shows the regular distribution of glass fiber inside the composites. It is found that the poly olefin polymer has been torn apart from the surface of the glass fiber, Composite 1, 2 (Figure 4a, b), which contains the amino silane and urethane as binders, and the interfacial surface is found to be very coarse and rough when the glass fiber fracture surface of composites is closely examined. Such phenomenon is attributed to the effective adhesion between the glass fiber and the polyolefin ketone polymer, the supportive matter, which in turn causes the polymer with low strength to be torn apart and left on the surface of the glass fiber.

By contrast, nearly no polymer is left on the surface of glass fiber, Composite 4, and the interfacial surface is very clean as shown in Fig. 4c. In the Composite 5 as shown in Fig. 4d, only small amount of polymer can be observed on the surface. Also, many holes are found, through which large quantities of glass fiber seemed to have passed. The holes – through which the fiber seems to have passed – have clean cross-sections, suggesting that the adhesion between the two matters is not effective. The increased compatibility

between the binder of glass fiber and polymer, i.e., the improvement of interfacial adhesion, is considered attributable to the increase in the polarity element which results from the hydrogen bond among respective matters[9]. In other words, the glass fiber that has additional epoxy component exhibits lower compatibility, compared to the fiber that contains only the urethane, because the surface area for the hydrogen bond with polyolefin ketone polymer becomes small, and such a decline in the compatibility is considered to have an impact on the mechanical properties of composites.

Mechanical properties of composites

The mechanical properties of polyolefin ketone terpolymer and glass fiber-reinforced composites, i.e., tensile strength, tensile modulus, elongation rate (elongation at break), flexural strength, flexural modulus, Charpy impact strength (Unnotched Charpy), etc., were measured using the universal testing machine (UTM). The results of the measurements are presented in the Table 2. Mechanical properties increased in all composites, except for the tensile elongation, regardless of the type of glass fiber. For the 910 type, three different types of glass fibers with different diameter and length of fiber were tested.

Although the results of the test showed that the length of the chopped strand did not have significant effect on the physical properties, the composite material (Composite 1) containing the glass fiber, of which diameter was increased from 10 μm to 13 μm , outperformed other materials in terms of mechanical properties. In particular, it was

found that such composite material (containing the glass fiber, of which diameter was increased from 10 μ m to 13 μ m) had the tensile modulus which was over 1000% and 250% higher compared to that of the copolymer and other composite materials, respectively. When varying the length of glass fiber when the diameter and binder of glass fiber were the same, the composites containing the 4mm glass fiber was found to show slightly higher measurement values in physical properties than the composites containing the 3mm glass fiber, except for the tensile modulus. However, overall mechanical properties of the composites were not affected significantly. Based on the comparison between Composite 2 and Composite 3 glass fibers that had same size but different binders, it was found that the tensile strength or flexural strength and tensile elongation were affected by the interfacial properties. Particularly, 923 type (Composite 4) had lower strength and tensile elongation compared to other composites, which is attributed to the ineffective adhesion between the glass fiber and the polymer as mentioned before.

Table 2 illustrates the mechanical properties of Composite 1-1 formed by the mixture of the low concentration (15 wt%) polymer and 910-13P-4 glass fiber which showed the most excellent performance. In addition, a comparison was made with the physical properties of the polyamide 6 polymer composites supplied by Kolon in order to determine the applicability in the engineering plastic fields. As shown in the Table 2, polyolefin ketone composites, if used at the same content level, provides the performance comparable to that of commercialized composites in terms of other physical properties

and exhibits over 200% higher tensile modulus and Charpy impact strength. Polyolefin ketone composites was found to deliver the performance similar to that of the composites that have bad interfacial properties, even if the glass fiber concentration was low, and exhibited far more excellent tensile modulus and therefore is considered to be able to find practical applications in the engineering plastic sector.

4.4. Conclusions

In this study, polyolefin ketone terpolymer with excellent mechanical properties was synthesized and the composites reinforced with various types of glass fibers were prepared, and the interfacial properties and mechanical properties in relation to the fibers were determined. The synthesis conditions suited for the mass production were identified, and the polymer with desired physical properties were obtained in large quantities by determining the correlation between the catalyst activity and intrinsic viscosity, depending on the polymerization temperature. Besides, the interfacial properties in relation to the polymer were identified, which varied depending on the length and diameter of the used glass fiber (used as enforcement) and the binder, and furthermore, the resultant changes in the mechanical properties were determined. The polymer, the subject of this study, has excellent mechanical properties and can be synthesized in large capacity, and delivers superior performance, compared to the current commercialized composites, through the combination with the glass fiber which it has excellent compatibility with. Thus, this polymer is considered to be applicable in the engineering plastic sector.

The results of the study are meaningful in that they presented the glass fiber-reinforced polyolefin ketone composites which have highly excellent mechanical properties and can be manufactured in large capacity.

Table 4-1. Characteristics of Glass Fibers used in this Work

Glass fiber	Fiber diameter (μm)	Chop length (mm)	Compatibility with poly(olefin ketone)
910-13P-4	13	4	O
910-10P-4	10	4	O
910-10P-3	10	3	O
923-10C-4	10	4	X
995-10P-4	10	4	Δ

Table 4-2. Mechanical Properties of Poly(olefin ketone) Terpolymer, Glass Fiber Reinforced Poly(olefin ketone) Composites, and Polyamide 6 Composite.

	Tensile strength (MPa)	Tensile modulus (MPa)	Elongation at break (%)	Flexural strength (MPa)	Flexural modulus (MPa)	Unnotched Charpy (KJ/m ²)
POK terpolymer	63	1900	25.0	65	1950	15.0
Composite 1 ^a	152	20500	3.4	215	8377	17.6
Composite 2 ^b	146	8000	3.3	200	6100	12.9
Composite 3 ^c	143	8100	3.1	196	5800	11.9
Composite 4 ^d	108	9035	1.6	148	6078	9.2
Composite 5 ^e	136	7800	3.1	187	5500	10.2
Composite 1-1 ^f	108	12500	5	149	4500	12.0
Polyamide6 +GF(30wt%) ^g	160	9600	2.7	223	8600	8.5

^a Poly(olefin ketone) composites containing 30 wt% of 910-13P-4, ^b 30 wt% of 910-10P-4, ^c 30 wt% of 910-10P-3, ^d 30 wt% of 923-10C-4, ^e 30 wt% of 995-10P-4, ^f 15 wt% of 910-13P-4.

^g Product information from Kolon Plastics, INC. (KOPA KN133G30BL)

Figure 4-1. Synthesis of poly(olefin ketone) terpolymer.

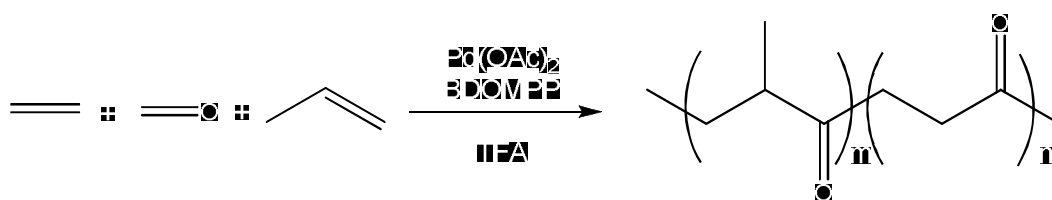


Figure 4-3. Palladium activity and intrinsic viscosity as a function of polymerization temperature

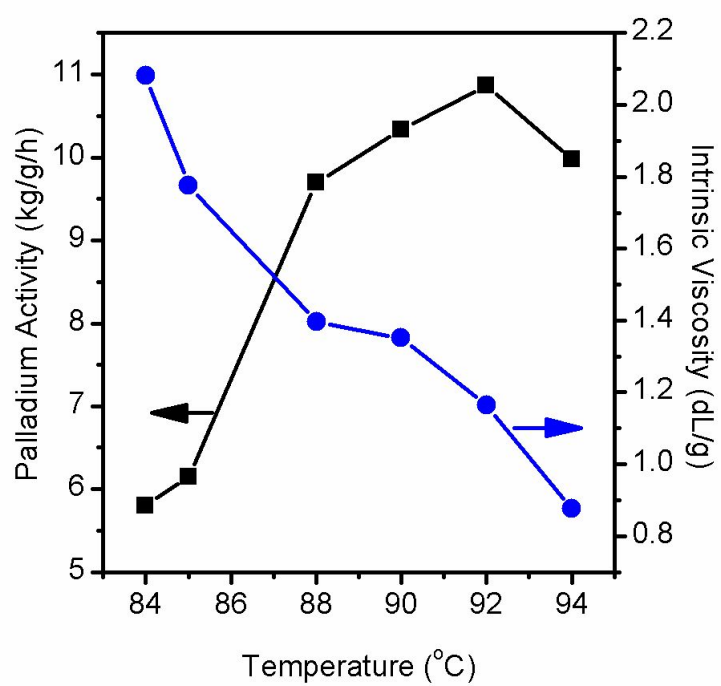
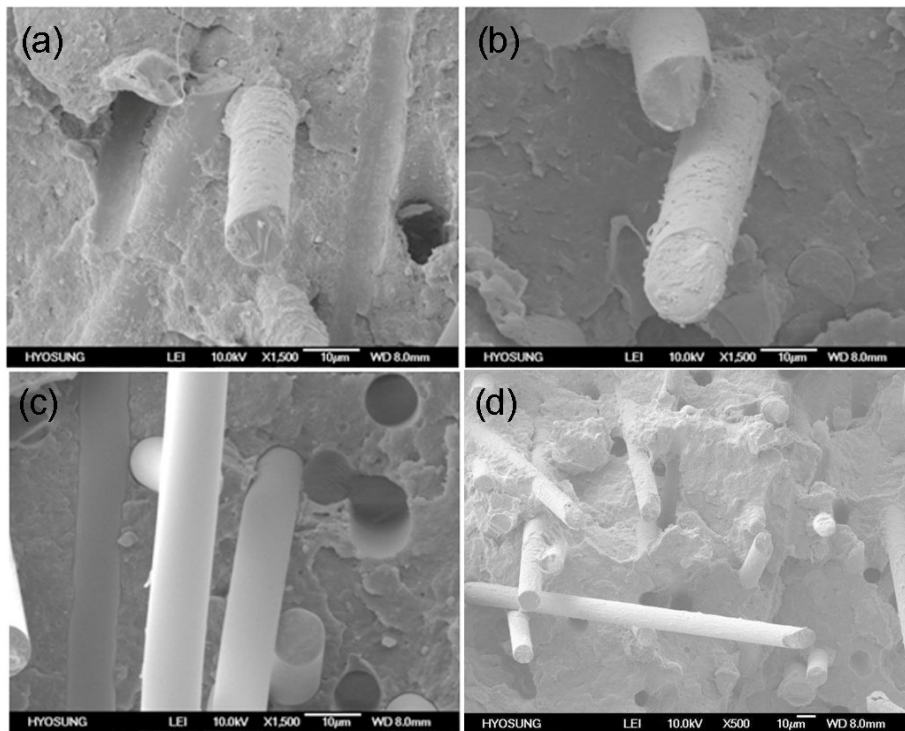


Figure 4-4. SEM images of glass fiber reinforced poly(olefin ketone) composites,
(a) Composite 1, (b) Composite 2, (c) Composite 4 and (d) Composite 5.



4.5. References

- [1] E. Drent, and P. H. M. Budzelaar, *Chem. Rev.*, 96(1996)663.
- [2] B. J. Lommerts, E. A. Klop, and J. Aerts, *J. Polym. Sci. B Polym. Phys.*, 31(1993)1319.
- [3] A. J. Waddon, N. R. Karttunen, and A. J. Lesser, *Macromolecules*, 32(1999)423.
- [4] A. J. Waddon, and N. R. Karttunen, *Macromolecules*, 35(2002) 4003.
- [5] T. Morita, R. Taniguchi, T. Matsuo, and J. Kato, *J. Appl. Polym. Sci.*, 92(2004)1183.
- [6] P. K. Mallick, *Fiber-reinforced Composites*, Marcel Dekker, New York, (1988).
- [7] J. W. Cho, and D. R. Paul, *Polymer*, 42(2001)1083.
- [8] J. S. Jang, *J. Korean Ind. Eng. Chem.*, 1(1990)133.
- [9] S.-J. Park, J.-X. Jin, and J.-R. Lee, *J. Korean Ind. Eng. Chem.*, 12(2001)143.
- [10] K. Na, H. S. Park, and H. Y. Won, *Macromol. Res.*, 14(2006)499.
- [11] J. H. Stephen, and N. J. Whippany, United States Patent No. 5034431 (1991).
- [12] S. K. Yoon, and H. S. Kim, Korea Patent No. 1020110078383 (2011).
- [13] H.-S. Cho, J.-S. Chung, J. Shim, J. Kim, W. J. Choi, and J.-C. Lee, *Macromol. Res.*, accepted (2012).

초 록

폴리올레핀케톤(IUPAC:Poly(1-oxotrimethylene)) 고분자는 일산화탄소와 올레핀 단량체의 교대 공중합으로 이루어져 있다. 이원 공중합물로 구성된 폴리케톤 고분자는 40년 넘게 잘 알려져 왔으나, 효과적인 합성방법은 최근에야 마련되었다. 또한 6wt% 프로필렌이 일산화탄소 및 에틸렌 반응에 참여한 삼원공중합 고분자도 개발되었다. 폴리케톤 고분자 합성과 관련한 종합인자들은 Shell사, BP사, 그리고 효성에 의해 개발 되어져 왔다. 본 연구에서는 잘 알려져 있는 반응메카니즘은 간단히 기술하고, 폴리케톤 상업화에 밀접한 고분자 고유점도, 분자량, 겔보기밀도와 직접적인 영향을 미치는 반응 온도와의 관계, 그리고 고유점도와 용융지수와의 직접적인 관계를 기술한다.

폴리올레핀케톤 이원공중합물을 중합하여 기계적 강도가 우수한 섬유를 제조하였고, 이를 열분석, X-ray 및 universal testing machine(UTM)으로 분석하였다. 분석결과, 16배 연신 시 13.4 and 369.8 g/denier의 인장강도 및 modulus를 가지고 있는 폴리올레핀케톤 섬유를 제조가 가능하였다. 이는 타이어코드에 범용으로 사용되는 poly(ethylene terephthalate) (PET) 와 나일론 6보다 우수한 물성으로 상업적 활용이 매우 높다.

우수한 기계적 강도를 가지고 있는 폴리올레핀케톤 고분자를 합성하고, 우레탄과 아미노실란으로 표면 처리 된 유리섬유를 도입하여 엔지니어링 플라스틱용 복합재료를 제조하였다. 유리섬유와 폴리올레핀케톤의 상용성을 확인하

기 위해 주사 전자 현미경으로 복합재료의 파단면 형상을 확인하였고, 함유된 유리섬유의 크기와 양, 그리고 바인더의 종류에 따른 복합재료의 기계적 물성을 관찰하였다. 적절한 표면처리를 한 유리섬유로 강화된 폴리올레핀케톤 복합재료는 좋은 계면 상용성을 보이며 향상된 기계적 강도를 가지고 엔지니어링 플라스틱 분야에서의 응용 가능성을 확인할 수 있었다.

주요어: 폴리올레핀케톤, 폴리(1-옥소트릴메틸렌), 섬유, 연신비, 결정화도, 유리섬유로 강화된 고분자

학번: 2007-30281